

# Waves in Nonlocal Elastic Solid with Voids

Dilbag Singh<sup>1,2</sup> · Gurwinderpal Kaur<sup>1</sup> · S.K. Tomar<sup>1</sup>

Received: 17 June 2016 / Published online: 9 January 2017  
© Springer Science+Business Media Dordrecht 2017

**Abstract** In this paper, the governing relations and equations are derived for nonlocal elastic solid with voids. The propagation of time harmonic plane waves is investigated in an infinite nonlocal elastic solid material with voids. It has been found that three basic waves consisting of two sets of coupled longitudinal waves and one independent transverse wave may travel with distinct speeds. The sets of coupled waves are found to be dispersive, attenuating and influenced by the presence of voids and nonlocality parameters in the medium. The transverse wave is dispersive but non-attenuating, influenced by the nonlocality and independent of void parameters. Furthermore, the transverse wave is found to face critical frequency, while the coupled waves may face critical frequencies conditionally. Beyond each critical frequency, the respective wave is no more a propagating wave. Reflection phenomenon of an incident coupled longitudinal waves from stress-free boundary surface of a nonlocal elastic solid half-space with voids has also been studied. Using appropriate boundary conditions, the formulae for various reflection coefficients and their respective energy ratios are presented. For a particular model, the effects of non-locality and dissipation parameter ( $\tau$ ) have been depicted on phase speeds and attenuation coefficients of propagating waves. The effect of nonlocality on reflection coefficients has also been observed and shown graphically.

**Keywords** Nonlocality · Voids · Elastic wave · Phase speed · Attenuation · Reflection

**Mathematics Subject Classification** 74J10 · 73B18 · 73D15 · 35Q74

---

✉ S.K. Tomar  
[sktomar66@gmail.com](mailto:sktomar66@gmail.com)

D. Singh  
[kahlondilbag@yahoo.com](mailto:kahlondilbag@yahoo.com)

G. Kaur  
[grewalgk1991@gmail.com](mailto:grewalgk1991@gmail.com)

<sup>1</sup> Department of Mathematics, Panjab University, Chandigarh 160 014, India

<sup>2</sup> University Grants Commission, New Delhi 110 002, India

## 1 Introduction

The theory of nonlocal elasticity has been studied by many researchers (see [1–3]). Ede- len and his co-workers [4–6] developed the nonlocal elasticity theories characterized by the presence of nonlocality residuals of fields (like body force, mass, entropy, internal energy, etc.) and determined these residuals, along with the constitutive laws, with the help of suitable thermodynamic restrictions. The concept of nonlocality has been extended to various other fields by Eringen [7–11], McCay and Narsimhan [12], Narsimhan and McCay [13]. In nonlocal theory of elasticity, the stress at any reference point  $\mathbf{x}$  within a continuous body depends not only on the strain at that point, but also significantly influenced by the strains at all other points  $\mathbf{x}'$  of the continuous body. Thus, the nonlocal stress forces act as a remote action forces. These types of forces are frequently encountered in atomic theory of lattice dynamics. Nonlocal continuum mechanics is now well established and is being applied to the problems of wave propagation (see [14, 15]). Using nonlocal continuum mechanics for modeling, the analysis of nanostructures has been made by several researchers, for example, Narendar and Gopalakrishnan [16, 17], Narendar et al. [18], Malagu et al. [19], etc.

The theory of elastic materials with voids developed by Cowin and his co-worker [20, 21] is a beautiful extension of the classical theory of elasticity. In their theory, the strain and the change in void volume fraction are considered as independent kinematic variables. Later, Puri and Cowin [22] studied the propagation of harmonic plane waves in a linear elastic material with voids and showed that there exist two dilatational waves and one transverse wave. One of the dilatational waves is predominantly dilatational wave of classical linear elasticity, while the second dilatational wave is predominantly a wave carrying a change in void volume fraction. Both the dilatational waves are found to attenuate in their direction of propagation. At large frequencies, the predominantly elastic wave propagates with the classical elastic dilatational wave speed, but at low frequency it propagates at a speed less than the classical wave speed. The transverse wave is found to travel with the speed of classical transverse wave and is not influenced by the presence of voids. Iesan [23] extended the Cowin's theory of elastic material with voids to incorporate thermal effect. He presented the basic field equations and investigated the condition of propagation of acceleration waves in a homogeneous isotropic thermo-elastic material with voids. He also showed that the transverse wave propagates without the influence of temperature and voids present in the medium. Using Iesan's theory, Singh and Tomar [24] investigated the propagation of plane waves in a thermo-elastic material with voids. They have also studied the reflection of plane waves against the stress-free insulated boundary of a thermo-elastic material half-space with voids. Recently, Iesan [25] further extended his earlier theory to include viscoelastic effect and presented constitutive relations and equations for linear theory of thermo-viscoelastic material with voids. By employing Iesan's theory, Tomar et al. [26], Sharma et al. [27] and D'Apice and Chirita [28] studied the propagation of plane waves in thermo-viscoelastic material with voids.

In the present paper, we have derived the constitutive relations for nonlocal elastic solid with voids using strain energy density function. Since the force stress tensor, equilibrated stress vector, and intrinsic equilibrated body force depend on the strains at all points of the body, therefore, these quantities are expressed in the form of integral over the entire volume of the body. The governing field equations for linear isotropic nonlocal elastic solid with voids are also derived and presented in compact form. The possibility of propagation of plane waves in an infinite isotropic, nonlocal elastic solid with voids has been investigated. It has been seen that there may exist three plane waves comprising of two sets of coupled longitudinal waves and one uncoupled transverse wave. Each set of coupled dilatational waves consist of a longitudinal displacement wave and a wave carrying the change in

void volume fraction. The phase speeds and corresponding attenuations of coupled longitudinal waves are found to be dependent on nonlocal parameter, elastic parameters, voids and frequency parameters. The transverse wave is found to be dispersive but non-attenuating. Thus, all the existing waves are not only dispersive but also influenced by the nonlocality of the medium. The formulae for amplitude ratios and energy ratios corresponding to various reflected waves have been presented when a set of coupled longitudinal waves strikes obliquely at the stress-free boundary surface of a nonlocal elastic solid half-space with voids.

Similar problem has been attempted in other types of generalized continuum theories such as in couple-stress theory by Graff and Pao [29], in micropolar theory by Parfitt and Eringen [30], and in strain-gradient theory by Gourgiotis et al. [31].

## 2 Field Equations and Constitutive Relations

Here, we shall extend the constitutive relations and field equations for nonlocal elastic material with voids without memory. For isothermal linear elastic solid with voids, the equations and relations are already developed by Cowin and Nunziato [21]. The basic idea behind the theory of elastic material with voids is that the mass density  $\rho$  is written as a product of matrix density  $\gamma$  and void volume fraction  $\nu$  ( $0 < \nu \leq 1$ ). The void volume fraction is a measure of volume change of bulk material arising from void compaction and distention. This enables to introduce a new independent kinematic variable  $\phi$  corresponding to change in void volume fraction and which depends on spatial coordinates  $\mathbf{x}$  and time  $t$ . If  $\nu_R$  denotes the void volume fraction at reference configuration, then  $\phi = \nu(\mathbf{x}, t) - \nu_R$ .

Consider an elastic body with voids having volume  $V$ , bounded by the surface  $S$  and occupying region  $\mathbb{B}$  in  $\mathbb{R}^3$  at time  $t_0$  of reference configuration. Let the position of a typical point of  $\mathbb{B}$  in undeformed state be  $X_i$  and the position of the corresponding point in the deformed state be  $x_i$ . The displacement vector  $u_i$  of the particle is given by  $u_i = x_i - X_i$ . Let us denote the strain tensor, gradient of void volume fraction by  $e_{ij}$  and  $\phi_{,i}$ , respectively. In the linear theory, the Lagrangian strain tensor reduces to

$$e_{ij} = \frac{1}{2}(u_{i,j} + u_{j,i}).$$

Within the context of linear theory, and assuming that the initial body is free from stresses and has zero intrinsic equilibrated force, we take the set of basic variables at points  $\mathbf{x}$  and  $\mathbf{x}'$ , respectively as

$$Y = \{e_{ij}(\mathbf{x}), \phi(\mathbf{x}), \phi_{,i}(\mathbf{x})\} \quad \text{and} \quad Y' = \{e_{ij}(\mathbf{x}'), \phi(\mathbf{x}'), \phi_{,i}(\mathbf{x}')\}.$$

The strain energy function  $U$  is given by

$$\begin{aligned} 2U = & C_{ijkl}e_{ij}(\mathbf{x})e_{kl}(\mathbf{x}') + \xi\phi(\mathbf{x})\phi(\mathbf{x}') + A_{ij}\phi_{,i}(\mathbf{x})\phi_{,j}(\mathbf{x}') + B_{ij}[e_{ij}(\mathbf{x})\phi(\mathbf{x}') \\ & + e_{ij}(\mathbf{x}')\phi(\mathbf{x})] + D_{ijk}[e_{ij}(\mathbf{x})\phi_{,k}(\mathbf{x}') + e_{ij}(\mathbf{x}')\phi_{,k}(\mathbf{x})] \\ & + d_i[\phi(\mathbf{x})\phi_{,i}(\mathbf{x}') + \phi(\mathbf{x}')\phi_{,i}(\mathbf{x})], \end{aligned} \tag{1}$$

where the constitutive coefficients  $C_{ijkl}$ ,  $\xi$ ,  $A_{ij}$ ,  $B_{ij}$ ,  $D_{ijk}$ , and  $d_i$  are prescribed functions of  $\mathbf{x}$  and  $\mathbf{x}'$ .

We adopt the following symmetries in the constitutive coefficients as

$$C_{ijkl}(\mathbf{x}, \mathbf{x}') = C_{klij}(\mathbf{x}, \mathbf{x}') = C_{jikl}(\mathbf{x}, \mathbf{x}'), \quad A_{ij}(\mathbf{x}, \mathbf{x}') = A_{ji}(\mathbf{x}, \mathbf{x}'),$$

$$B_{ij}(\mathbf{x}, \mathbf{x}') = B_{ji}(\mathbf{x}, \mathbf{x}'), \quad D_{ijk}(\mathbf{x}, \mathbf{x}') = D_{jik}(\mathbf{x}, \mathbf{x}').$$

Following Eringen [32], the constitutive relations are obtained from

$$\Gamma = \int_V \left[ \frac{\partial U}{\partial Y} + \left( \frac{\partial U}{\partial Y'} \right)^s \right] dV(\mathbf{x}'),$$

where the superscript ‘s’ represents the symmetry of that quantity with respect to interchange of  $\mathbf{x}$  and  $\mathbf{x}'$ . The set  $\Gamma = \{t_{ij}, F - g, h_i\}$  is an ordered set with the set  $Y$ . Here, the function  $F$  is a dissipation function given by

$$F = - \int_V \tau(\mathbf{x}, \mathbf{x}') \dot{\phi}(\mathbf{x}') dV(\mathbf{x}'), \tag{2}$$

where non-negative coefficient  $\tau$  is a constitutive coefficient and superposed dot denotes the time derivative. Thus, the force stress tensor  $t_{ij}$ , equilibrated stress vector  $h_i$  and equilibrated body force  $g$  are obtained as

$$t_{ij} = \int_V [C_{ijkl}(\mathbf{x}, \mathbf{x}') e_{kl}(\mathbf{x}') + B_{ij}(\mathbf{x}, \mathbf{x}') \phi(\mathbf{x}') + D_{ijk}(\mathbf{x}, \mathbf{x}') \phi_{,k}(\mathbf{x}')] dV(\mathbf{x}'), \tag{3}$$

$$h_i = \int_V [D_{kli}(\mathbf{x}, \mathbf{x}') e_{kl}(\mathbf{x}') + d_i(\mathbf{x}, \mathbf{x}') \phi(\mathbf{x}') + A_{ij}(\mathbf{x}, \mathbf{x}') \phi_{,j}(\mathbf{x}')] dV(\mathbf{x}'), \tag{4}$$

$$g = - \int_V [\tau(\mathbf{x}, \mathbf{x}') \dot{\phi}(\mathbf{x}') + \xi(\mathbf{x}, \mathbf{x}') \phi(\mathbf{x}') + B_{ij}(\mathbf{x}, \mathbf{x}') e_{ij}(\mathbf{x}') + d_i(\mathbf{x}, \mathbf{x}') \phi_{,i}(\mathbf{x}')] dV(\mathbf{x}'). \tag{5}$$

For a centro-symmetric isotropic material, the constitutive coefficients are given by

$$C_{ijkl} = \lambda(\mathbf{x}, \mathbf{x}') \delta_{ij} \delta_{kl} + 2\mu(\mathbf{x}, \mathbf{x}') \delta_{ik} \delta_{jl}, \quad D_{ijk} = 0,$$

$$A_{ij} = \alpha(\mathbf{x}, \mathbf{x}') \delta_{ij}, \quad B_{ij} = \beta(\mathbf{x}, \mathbf{x}') \delta_{ij}, \quad d_i = 0,$$

where the coefficients  $\lambda, \mu, \alpha, \beta, \tau$  and  $\xi$  are functions of  $|\mathbf{x} - \mathbf{x}'|$ , that is,  $\alpha = \alpha(|\mathbf{x} - \mathbf{x}'|)$ ,  $\beta = \beta(|\mathbf{x} - \mathbf{x}'|)$ , etc. Thus, the constitutive relations (3)–(5) become

$$t_{ij} = \int_V [\lambda(|\mathbf{x} - \mathbf{x}'|) \delta_{ij} e_{kk}(\mathbf{x}') + 2\mu(|\mathbf{x} - \mathbf{x}'|) e_{ij}(\mathbf{x}') + \beta(|\mathbf{x} - \mathbf{x}'|) \phi(\mathbf{x}') \delta_{ij}] dV(\mathbf{x}'), \tag{6}$$

$$h_i = \int_V \alpha(|\mathbf{x} - \mathbf{x}'|) \phi_{,i}(\mathbf{x}') dV(\mathbf{x}'), \tag{7}$$

$$g = - \int_V [\tau(|\mathbf{x} - \mathbf{x}'|) \dot{\phi}(\mathbf{x}') + \xi(|\mathbf{x} - \mathbf{x}'|) \phi(\mathbf{x}') + \beta(|\mathbf{x} - \mathbf{x}'|) e_{kk}(\mathbf{x}')] dV(\mathbf{x}'). \tag{8}$$

For most of the materials, the cohesive zone is very small, and within that zone the intermolecular forces decrease rapidly with distance from the reference point. Hence, we consider that all the constitutive coefficients attenuate with distance, e.g.,

$$\lim_{(|\mathbf{x} - \mathbf{x}'|) \rightarrow \infty} \lambda(|\mathbf{x} - \mathbf{x}'|) \rightarrow 0.$$

We also consider that all the constitutive coefficients attenuate with same degree and they attain their maxima at  $\mathbf{x} = \mathbf{x}'$ . Therefore, we can take the following relations between non-local and local elastic coefficients

$$\begin{aligned} \frac{\lambda(|\mathbf{x} - \mathbf{x}'|)}{\lambda_0} &= \frac{\mu(|\mathbf{x} - \mathbf{x}'|)}{\mu_0} = \frac{\alpha(|\mathbf{x} - \mathbf{x}'|)}{\alpha_0} = \frac{\beta(|\mathbf{x} - \mathbf{x}'|)}{\beta_0} \\ &= \frac{\xi(|\mathbf{x} - \mathbf{x}'|)}{\xi_0} = \frac{\tau(|\mathbf{x} - \mathbf{x}'|)}{\tau_0} = G(|\mathbf{x} - \mathbf{x}'|). \end{aligned} \tag{9}$$

Here, the quantities in the denominator are constant coefficients. The  $\lambda_0, \mu_0$  are the well known Lamé’s constants;  $\alpha_0, \beta_0, \xi_0$ , and  $\tau_0$  are constants corresponding to voids and the function  $G(|\mathbf{x} - \mathbf{x}'|)$  is a non-local kernel representing the effect of distant interactions of material points between  $\mathbf{x}'$  and  $\mathbf{x}$ . Also, the integral of non-local kernel  $G(|\mathbf{x} - \mathbf{x}'|)$  over the domain of integration is unity, i.e.,

$$\int_V G(|\mathbf{x} - \mathbf{x}'|)dV = 1.$$

Hence, the kernel function  $G$  behaves as a Dirac-delta function over the domain of influence. The function  $G$  attains its peak at  $|\mathbf{x} - \mathbf{x}'| = 0$  and generally decays with increasing  $|\mathbf{x} - \mathbf{x}'|$ . Eringen [33] has already shown that the function  $G$  satisfies the relation

$$(1 - \epsilon^2 \nabla^2)G = \delta(|\mathbf{x} - \mathbf{x}'|), \tag{10}$$

where  $\epsilon = e_0 a$  is a non-local parameter,  $a$  being the internal characteristic length and  $e_0$  is a material constant. The internal characteristic length  $a$  is the interatomic distance, e.g., length of C–C bond (0.142 nm in Carbon nanotube).

Applying the operator  $(1 - \epsilon^2 \nabla^2)$  on the constitutive relations (6)–(8), owing to the relation (9) and the property (10), we obtain (after suppressing the subscript ‘0’ from the constitutive coefficients)

$$(1 - \epsilon^2 \nabla^2)t_{ij} = t_{ij}^L = \lambda \delta_{ij} e_{kk}(\mathbf{x}) + 2\mu e_{ij}(\mathbf{x}) + \beta \delta_{ij} \phi(\mathbf{x}), \tag{11}$$

$$(1 - \epsilon^2 \nabla^2)h_i = h_i^L = \alpha \phi_{,i}(\mathbf{x}), \tag{12}$$

$$(1 - \epsilon^2 \nabla^2)g = g^L = -\tau \dot{\phi}(\mathbf{x}) - \xi \phi(\mathbf{x}) - \beta e_{kk}(\mathbf{x}), \tag{13}$$

wherein the formula

$$\int f(x)\delta(x - a)dx = f(a),$$

has been employed. Here, the quantities  $t_{ij}^L, h_i^L, g^L$  correspond to local elastic solid material with voids.

Cowin and Nunziato [21] have already derived the following restrictions among various material parameters as

$$\mu \geq 0, \quad \alpha \geq 0, \quad \xi \geq 0, \quad 3\lambda + 2\mu \geq 0, \quad (3\lambda + 2\mu)\xi \geq 3\beta^2.$$

Note that a correction pointed out by Puri and Cowin [22] has been taken care here.

Equations of motion for a non-local isotropic elastic solid with voids are given by

$$t_{ij,j} + \rho(f_i - \ddot{u}_i) = 0, \tag{14}$$

$$h_{i,i} + g + \rho(l - \chi\ddot{\phi}) = 0, \tag{15}$$

where  $f_i$  is the body force,  $l$  is the extrinsic equilibrated body force,  $\chi$  is the equilibrated inertia and  $\rho$  is the bulk density. Superposed dots represent the double time derivative and comma (,) in the subscript represents the spatial partial derivative.

Plugging the constitutive relations (11)–(13) into (14) and (15), we obtain the following equations

$$\beta\nabla\phi + (\lambda + 2\mu)\nabla(\nabla \cdot \mathbf{u}) - \mu\nabla \times (\nabla \times \mathbf{u}) + \rho(1 - \epsilon^2\nabla^2)(\mathbf{f} - \ddot{\mathbf{u}}) = \mathbf{0}, \tag{16}$$

$$\alpha\nabla^2\phi - \xi\phi - \beta\nabla \cdot \mathbf{u} - \tau\dot{\phi} + \rho(1 - \epsilon^2\nabla^2)(l - \chi\ddot{\phi}) = 0. \tag{17}$$

These are the equations of small motion in a nonlocal isotropic elastic solid with voids. Note that in the absence of non-locality, that is, when  $\epsilon = 0$ , these equations reduce to those of local isotropic elastic solid with voids earlier derived by Puri and Cowin [22].

### 3 Wave Propagation

Introducing the scalar and vector potentials  $q$  and  $\mathbf{U}$  through Helmholtz decomposition theorem on vectors as

$$\mathbf{u} = \nabla q + \nabla \times \mathbf{U}, \quad \nabla \cdot \mathbf{U} = 0. \tag{18}$$

With the help of (18), Eqs. (16) and (17), in the absence of body force densities, reduce to

$$\beta\phi + (\lambda + 2\mu)\nabla^2 q - \rho(1 - \epsilon^2\nabla^2)\ddot{q} = 0, \tag{19}$$

$$\mu\nabla^2\mathbf{U} - \rho(1 - \epsilon^2\nabla^2)\ddot{\mathbf{U}} = \mathbf{0}, \tag{20}$$

$$\alpha\nabla^2\phi - \xi\phi - \tau\dot{\phi} - \beta\nabla^2 q - \rho(1 - \epsilon^2\nabla^2)\chi\ddot{\phi} = 0. \tag{21}$$

We note that (19) and (21) are coupled in potentials  $q$  and  $\phi$ , while (20) is uncoupled in potential  $\mathbf{U}$ .

For a plane wave propagating in the positive direction of unit vector  $\mathbf{n}$  with speed  $c$  through nonlocal elastic solid with voids, we can take

$$\{\phi, q, \mathbf{U}\} = \{a_1, b_1, \mathbf{B}_1\} \exp\{ik(\mathbf{n} \cdot \mathbf{r} - ct)\}, \tag{22}$$

where  $a_1, b_1$  are scalar constants,  $\mathbf{B}_1$  is vector constant,  $\mathbf{r} (= x\hat{i} + y\hat{j} + z\hat{k})$  is the position vector and  $k$  is the wavenumber. The wavenumber  $k$  and wave speed  $c$  are connected with angular frequency  $\omega$  through the relation  $\omega = kc$ .

Plugging the expressions of  $q$  and  $\phi$  from (22) into (19) and (21), we obtain

$$\beta a_1 - [(\lambda + 2\mu) - \rho c^2(1 + k^2\epsilon^2)]k^2 b_1 = 0, \tag{23}$$

$$[\rho k^2(1 + \epsilon^2 k^2)\chi - \alpha k^2 - \xi + i\tau kc]a_1 + \beta k^2 b_1 = 0. \tag{24}$$

These equations are system of two homogeneous equations in two unknowns, namely,  $a_1$  and  $b_1$ . For a non-trivial solution of homogeneous system of equations (23) and (24), the

determinant of coefficient matrix must be equal to zero. This yields us a quadratic equation in  $c^2$  given by

$$Ac^4 + Bc^2 + C = 0, \tag{25}$$

where

$$\begin{aligned} A &= \rho(\rho\chi\omega^2 + i\tau\omega - \xi), \\ B &= 2\rho^2\epsilon^2\chi\omega^4 + i\tau\rho\epsilon^2\omega^3 - \rho[\chi(\lambda + 2\mu) + \alpha + \epsilon^2\xi]\omega^2 \\ &\quad + (\lambda + 2\mu)(\xi - i\tau\omega) - \beta^2, \\ C &= \rho^2\chi\epsilon^4\omega^6 - \rho\epsilon^2[\chi(\lambda + 2\mu) + \alpha]\omega^4 + \alpha(\lambda + 2\mu)\omega^2. \end{aligned} \tag{26}$$

The coefficients in (26) may be rearranged as

$$\begin{aligned} A &= \rho^2\chi(\omega^2 + i\ell_2^2\omega - \ell_1^2), \\ B &= \rho^2\epsilon^2\chi[2\omega^4 + i\ell_2^2\omega^3 - (\omega_{c_1}^2 + \omega_{c_2}^2 + \ell_1^2)\omega^2 - i\omega_{c_1}^2\ell_2^2\omega + \omega_{c_1}^2\ell_1^2] - \beta^2, \\ C &= \rho^2\chi\epsilon^4\omega^2(\omega^2 - \omega_{c_1}^2)(\omega^2 - \omega_{c_2}^2), \end{aligned} \tag{27}$$

where

$$\omega_{c_1}^2 = \frac{c_l^2}{\epsilon^2}, \quad \omega_{c_2}^2 = \frac{c_v^2}{\epsilon^2}, \quad c_l^2 = \frac{\lambda + 2\mu}{\rho}, \quad c_v^2 = \frac{\alpha}{\rho\chi}, \quad \ell_1^2 = \frac{\xi}{\rho\chi}, \quad \ell_2^2 = \frac{\tau}{\rho\chi}.$$

Note that for real  $\omega$ , the coefficients  $A$  and  $B$  are complex, while the coefficient  $C$  is real. The two roots of quadratic equation (25) are given by

$$c_{1,2}^2 = \frac{1}{2A}(-B \mp \sqrt{B^2 - 4AC}). \tag{28}$$

Here  $c_1^2$  corresponds to ‘-’ sign and  $c_2^2$  corresponds to ‘+’ sign. The values of  $c_1$  and  $c_2$  represent the speeds of two propagating waves. Since  $q$  and  $\phi$  are coupled through (19) and (21), therefore from (23) and (24), we obtain

$$a_1 = \zeta b_1, \tag{29}$$

where  $\zeta$  is the coupling coefficient given by

$$\zeta = \frac{(c_l^2 - c^2 - \epsilon^2\omega^2)\rho\omega^2}{\beta c^2} = \frac{-\beta\rho\omega^2}{Ac^2 + \rho\omega^2(\rho\epsilon^2\omega^2\chi - \alpha)}, \tag{30}$$

where  $c_l$  has been defined earlier and represents the speed of classical longitudinal wave.

Now, plugging the expression of  $\mathbf{U}$  from (22) into (20), we get

$$c_3^2 = c_t^2 - \epsilon^2\omega^2, \tag{31}$$

where  $c_t = \sqrt{\mu/\rho}$ , is the speed of classical transverse wave. Clearly, the wave traveling with speed  $c_3$  is independent of void parameters and travels slower than that in classical continuum. This reduction in the speed of transverse wave is due to the presence of nonlocality in the medium.

It is clear that the waves propagating with speeds  $c_i$  ( $i = 1, 2, 3$ ) are all dispersive in nature as they depend upon frequency  $\omega$ . The presence of nonlocality parameter  $\epsilon$  in the expressions of their speeds shows that these waves are influenced by the nonlocality of the medium.

Inserting  $q$  from (22) into (18), the displacement vector  $\mathbf{u}$  can be written as

$$\mathbf{u} = ikb_1 \mathbf{n} \exp\{ik(\mathbf{n} \cdot \mathbf{r} - ct)\}. \tag{32}$$

This shows that the vector  $\mathbf{u}$  is parallel to the vector  $\mathbf{n}$ . Thus, the particle motion associated with potential  $q$  is in the direction of wave propagation. Hence, the wave propagating with speed  $c_1$  is longitudinal in nature and we shall call it as *longitudinal displacement wave*. From relations (29) and (32), we observe that the wave associated with  $\phi$  is also longitudinal in nature and is called as *void volume fraction wave*. Similarly, inserting  $\mathbf{U}$  from (22) into (18), one can see that the particle motion associated with potential  $\mathbf{U}$  is normal to the direction of wave propagation  $\mathbf{n}$  and hence, the corresponding wave propagating with speed  $c_3$  is *transverse* in nature.

It can be noticed that the expressions of speeds  $c_i$  ( $i = 1, 2$ ) will be complex, hence the corresponding waves are attenuating. The phase speed  $V_i$  ( $i = 1, 2, 3$ ) and corresponding attenuation coefficient  $Q_i$  of the attenuating waves are given by (see Borchardt [34])

$$V_i = \frac{(\Re(c_i))^2 + (\Im(c_i))^2}{\Re(c_i)}, \tag{33}$$

$$Q_i = \frac{-\omega \Im(c_i)}{(\Re(c_i))^2 + (\Im(c_i))^2}, \tag{34}$$

where  $\Re(\cdot)$  and  $\Im(\cdot)$  represent the real and imaginary parts.

### 3.1 Further Discussion

Here, we wish to investigate the frequency range for propagating waves in the medium. To find out the frequency range for transverse wave traveling with speed  $c_3$ , we see from (31) that  $c_3 = 0$  at  $\omega = \omega_{c_3}$  ( $= c_1/\epsilon$ ). For  $\omega > \omega_{c_3}$ , we observe that the speed  $c_3$  will be purely imaginary. Thus, we can declare that this wave is propagating wave for the frequency range:  $0 \leq \omega < \omega_{c_3}$ . Beyond  $\omega = \omega_{c_3}$ , the wave is no more a propagating wave.

To find out the frequency range for propagating coupled longitudinal waves, we can notice from (27) that the coefficient  $C$  will vanish at  $\omega = \omega_{c_1}$  and  $\omega = \omega_{c_2}$  (provided  $\epsilon \neq 0$ ).

At the frequency  $\omega = \omega_{c_1}$ , one can easily check that the real part of  $B$  is negative, while the imaginary part of  $B$  is zero. Therefore from (28), we obtain that

$$c_1^2 = 0 \quad \text{and} \quad c_2^2 = \frac{\beta^2 + \rho^2 \epsilon^2 \chi \omega_{c_1}^2 (\omega_{c_2}^2 - \omega_{c_1}^2)}{\rho^2 \chi (\omega_{c_1}^2 + \iota \ell_2^2 \omega_{c_1} - \ell_1^2)}.$$

This means that one set of the coupled waves traveling with speed  $c_1$  disappears, while the other one travels with complex speed  $c_2$ .

At the frequency  $\omega = \omega_{c_2}$ , one can check that the coefficient  $B$  is complex and from (28), we see that

$$c_1^2 = \frac{\beta^2 + \rho \epsilon^2 (\omega_{c_2}^2 - \omega_{c_1}^2) (\xi - \rho \chi \omega_{c_2}^2 - \iota \tau \omega_{c_2})}{\rho^2 \chi (\omega_{c_2}^2 + \iota \ell_2^2 \omega_{c_2} - \ell_1^2)} \quad \text{and} \quad c_2^2 = 0.$$



This means that one set of the coupled waves traveling with speed  $c_2$  disappears, while the other set of coupled waves travels with complex speed  $c_1$ . Thus, at each frequency  $\omega_{c_1}$ , there exist only one set of coupled longitudinal waves propagating with complex speed. This fact has also been verified numerically through Fig. 11a.

It is clear from the expression of  $C$  given in (27) that for  $\omega > 0$  and  $\omega_{c_1} < \omega_{c_2}$ , the quantity  $C$  becomes negative in the range given by

$$\omega_{c_1} < \omega < \omega_{c_2},$$

and non-negative outside this range. In the entire range of frequency, the values of  $c_i$  are given by (28). In the entire frequency range  $0 < \omega < \infty$ , both the coupled waves propagate with complex speeds, except at frequency points  $\omega = \omega_{c_1}, \omega_{c_2}$  where only one set of coupled longitudinal waves exist.

*Remark* Note that the frequencies  $\omega_{c_i}$  ( $i = 1, 2$ ) may act as critical frequencies for the corresponding waves, if the real part of the speed is zero or very-very small and imaginary part is non-zero for  $\omega > \omega_{c_i}$ . For example, suppose for the range  $\omega > \omega_{c_1}$ , the wave traveling with complex speed  $c_1$  has its real part zero (or very-very small in magnitude) then clearly the speed of this wave will be purely imaginary. In such a case, it would not be a propagating wave and represents merely a distance decaying vibrations. In this situation,  $\omega = \omega_{c_1}$  will act as a critical frequency for the wave traveling with speed  $c_1$ .

A similar analysis can be made for the case when  $\omega_{c_1} > \omega_{c_2}$ .

Now, let us look at the behavior of the speeds of different waves at limitly low and high frequencies.

For limitly low frequency, i.e., when  $\omega \rightarrow 0$ , we note from (28) and (31) that

- (i) the limiting values of speeds  $c_1$  and  $c_2$  become

$$c_1 = \sqrt{c_l^2 - \frac{\beta^2}{\rho \xi}}, \quad \text{and} \quad c_2 = 0.$$

This shows that in the limitly low frequency case, one set of the coupled longitudinal waves disappears. The speed of remaining set of coupled longitudinal displacement waves is less than the speed of classical longitudinal wave. This reduction in the speed of coupled longitudinal waves is due the presence of voids in the medium.

- (ii) the speed  $c_3$  becomes

$$c_3 = \sqrt{\frac{\mu}{\rho}},$$

which is equal to the speed of classical shear wave ( $c_t$ ).

For limitly high frequency, i.e., when  $\omega \rightarrow \infty$ , one can see from (31) that the speed of transverse wave  $c_3$  decreases first with increase of  $\omega$  and goes to zero at  $\omega = \omega_{c_3}$ . Beyond  $\omega = \omega_{c_3}$ , the speed  $c_3$  becomes purely imaginary and the absolute value of which goes on increasing with further increase of  $\omega$ . From (28), we see that beyond  $\omega = \omega_{c_i}$  ( $i = 1, 2$ ) the absolute values of  $c_i$ , go on increasing with further increase of frequency as one can check that both  $c_1$  and  $c_2$  are proportional to  $\omega$ .

### 3.2 Special Cases

#### 3.2.1 Nonlocal Non-voigt Elastic Solid

A material with voids is said to be non-voigt, if its viscous type behavior is absent, that is,  $\tau = 0$ . In this case, (25) reduces to

$$A^*c^4 + B^*c^2 + C^* = 0,$$

where the coefficients  $A^*$ ,  $B^*$  and  $C^*$  are given by

$$A^* = \chi\omega^2 - \frac{\xi}{\rho}, \quad B^* = 2\epsilon^2\chi\omega^4 - \left(\chi c_l^2 + \frac{\alpha}{\rho} + \epsilon^2\frac{\xi}{\rho}\right)\omega^2 + \frac{\xi}{\rho}c_l^2 - \left(\frac{\beta}{\rho}\right)^2,$$

$$C^* = \chi\epsilon^4\omega^6 - \epsilon^2\left(\chi c_l^2 + \frac{\alpha}{\rho}\right)\omega^4 + \frac{\alpha}{\rho}c_l^2\omega^2.$$

Now we see that all the coefficients are real in nature. The roots of this quadratic equation will provide us the speeds of two waves, which are given by

$$c_{1,2}^2 = \frac{1}{2A^*}(-B^* \mp \sqrt{B^{*2} - 4A^*C^*}).$$

In the present case, it is easy to see that the waves having speeds  $c_{1,2}$  are dispersive. For their corresponding speeds to be real, the roots  $c_{1,2}^2$  must be real and positive, for which the discriminant ( $B^{*2} - 4A^*C^*$ ) must be positive. The positiveness can be checked keeping in view that the order of nonlocality is very small and the frequency is not too high. From the expression of  $A^*$ , we note that the quantity  $A^* > < 0$  accordingly as  $\omega > < \omega_c$  ( $= \sqrt{\xi/\rho\chi}$ ).

At  $\omega = \omega_c$ , we see that

$$\lim_{\omega \rightarrow \omega_c} c_1^2 = \left[ c_l^2 \left( 1 - \frac{\epsilon^2 \xi}{\alpha} \right) + \frac{\epsilon^2 \xi}{\alpha \rho \chi} (\xi - \alpha) \right] \left[ 1 - \frac{\epsilon^2 \xi}{\alpha} + \frac{\beta^2 \chi}{\alpha \xi} \right]^{-1},$$

and  $c_2^2 \rightarrow \infty$ . This means that at  $\omega = \omega_c$ , the wave speed  $c_1$  is finite and  $c_2$  has point of infinite discontinuity as also has been verified numerically through Fig. 12b.

As the coefficient  $C$  in (27) is independent of the constitutive coefficient  $\tau$ , therefore, the same frequencies  $\omega_{c_i}$  exist in this case also (see Sect. 3.1). Consequently, we conclude that in the frequency range  $\omega > \omega_{c_i}$  ( $i = 1, 2, 3$ ) the behavior of speeds of waves in nonlocal voigt ( $\tau \neq 0$ ) and non-voigt ( $\tau = 0$ ) elastic medium with voids remains same.

It can be seen easily that in the absence of nonlocality,  $\omega_{c_i} \rightarrow \infty$  for all  $i = 1, 2, 3$ . Thus, we conclude that in local elastic solid with voids, the waves with speed  $c_1$  and  $c_3$  will exist for all values of frequency, while the wave with speed  $c_2$  will still face a cut-off frequency at  $\omega = \sqrt{\xi/\rho\chi}$ , below which it is distance decaying vibrations only and beyond cut-off frequency it is a propagating wave.

#### 3.2.2 Local Elastic Solid with Voids

If we assume that the nonlocality is absent from the medium, then we shall be left with elastic medium with voids only. Putting nonlocality parameter, that is,  $\epsilon = 0$ , (25) becomes

$$Ac^4 + \bar{B}c^2 + \bar{C} = 0,$$

where  $A$  has already been defined and

$$\bar{B} = -(\rho\alpha\omega^2 + \beta^2 + c_l^2 A), \quad \bar{C} = \alpha\omega^2(\lambda + 2\mu).$$

In this case, the speeds of coupled longitudinal waves reduce to

$$c_{1,2}^2 = \frac{1}{2A}(-\bar{B} \mp \sqrt{\bar{B}^2 - 4A\bar{C}}),$$

and the speed of transverse wave, i.e.,  $c_3$  becomes equal to the classical shear wave speed ( $c_t$ ). These expressions of speeds are exactly same as obtained by Puri and Cowin [22].

### 3.2.3 Nonlocal Elastic Solid Without Voids

If we neglect the presence of void parameters, then we shall be left with nonlocality only in the medium. In this case, the speeds of coupled longitudinal waves reduce to

$$c_1 = \sqrt{c_l^2 - \epsilon^2\omega^2} \quad \text{and} \quad c_2 = 0,$$

and the speed of the transverse wave remains same, i.e.,  $c_3 = \sqrt{c_t^2 - \epsilon^2\omega^2}$  as this speed is independent of void parameters. We observe that in the absence of voids, i.e., when only nonlocality is present in the medium, the square of the speeds of longitudinal and transverse waves are frequency dependent and reduce by an amount equal to  $\epsilon^2\omega^2$ . At  $\omega = \omega_{c_1}$ , the longitudinal wave ceases to propagate, while at  $\omega = \omega_{c_3}$ , the transverse wave ceases to propagate. The frequencies  $\omega = \omega_{c_i}$  ( $i = 1, 3$ ) also act as critical frequencies for respective waves, beyond which the waves are no more propagating waves.

### 3.2.4 Classical Elastic Solid

If we neglect the nonlocality and void parameters together from the medium, we see that the speeds of coupled longitudinal waves reduce to  $c_1 = c_l$  and  $c_2 = 0$ , while the speed of the transverse wave reduces to  $c_3 = c_t$ . Thus, all the waves of classical elasticity are successfully recovered as was expected beforehand.

## 4 Reflection Phenomenon

Let  $OX_1X_2X_3$  be the cartesian coordinate system. We consider a nonlocal uniform elastic half-space with voids occupied by the region  $M = \{(x_1, x_2, x_3); -\infty < x_1, x_2 < \infty, 0 \leq x_3 < \infty\}$  such that  $x_3 = 0$  be the plane boundary surface of  $M$  and  $x_3$ -axis is pointing vertically downward into  $M$ . The boundary surface  $x_3 = 0$  of the half-space  $M$  is assumed to be free from mechanical stresses. For a two-dimensional problem in  $x_1$ - $x_3$  plane, we take

$$\mathbf{u} = (u_1, 0, u_3), \quad \frac{\partial}{\partial x_2} \equiv 0,$$

and from (18), we have

$$u_1 = q_{,1} - U_{2,3} \quad \text{and} \quad u_3 = q_{,3} + U_{2,1}, \tag{35}$$

where  $U_2$  is the  $x_2$  component of the vector  $\mathbf{U}$ .

Let a train of coupled longitudinal displacement waves having amplitude  $A_0$  and traveling with phase speed  $V_1$  is made incident making an angle  $\theta_0$  with the normal to the free surface  $x_3 = 0$ . In order to satisfy the boundary conditions at the free surface, we postulate the existence of following reflected waves:

- (i) A set of coupled longitudinal waves of amplitude  $A_1$  traveling with phase speed  $V_1$  and making an angle  $\theta_1$  with the normal.
- (ii) A similar set of coupled longitudinal waves of amplitude  $A_2$  traveling with phase speed  $V_2$  and making an angle  $\theta_2$  with the normal.
- (iii) A transverse wave of amplitude  $A_3$  traveling with phase speed  $V_3$  and making an angle  $\theta_3$  with the normal.

The total wave field in the half-space  $M$  can be expressed as

$$q = A_0 \exp\{ik_1(\sin \theta_0 x_1 - \cos \theta_0 x_3) - i\omega_1 t\} + \sum_{p=1,2} A_p \exp\{ik_p(\sin \theta_p x_1 + \cos \theta_p x_3) - i\omega_p t\}, \tag{36}$$

$$\phi = \zeta_1 A_0 \exp\{ik_1(\sin \theta_0 x_1 - \cos \theta_0 x_3) - i\omega_1 t\} + \sum_{p=1,2} \zeta_p A_p \exp\{ik_p(\sin \theta_p x_1 + \cos \theta_p x_3) - i\omega_p t\}, \tag{37}$$

$$U_2 = A_3 \exp\{ik_3(\sin \theta_3 x_1 + \cos \theta_3 x_3) - i\omega_3 t\}, \tag{38}$$

where  $\omega_i = k_i V_i$  ( $i = 1, 2, 3$ ).

To satisfy the boundary conditions at the free surface, we shall assume that  $\omega_1 = \omega_2 = \omega_3$  and

$$k_1 \sin \theta_0 = k_1 \sin \theta_1 = k_2 \sin \theta_2 = k_3 \sin \theta_3 = k_0 \text{ (say),}$$

or equivalently (Snell’s law)

$$\frac{V_1}{\sin \theta_0} = \frac{V_1}{\sin \theta_1} = \frac{V_2}{\sin \theta_2} = \frac{V_3}{\sin \theta_3} = v, \tag{39}$$

where ‘ $v$ ’ is the apparent velocity.

From Snell’s law (39), we find that  $\theta_0 = \theta_1$ , and the other angles of reflection depend upon the phase speeds  $V_1, V_2$  and  $V_3$  which are functions of material parameters. The complete geometry of the problem is shown in Fig. 1.

The quantity  $\zeta_i$  ( $i = 1, 2$ ) is the coupling coefficient (see (30)) given as

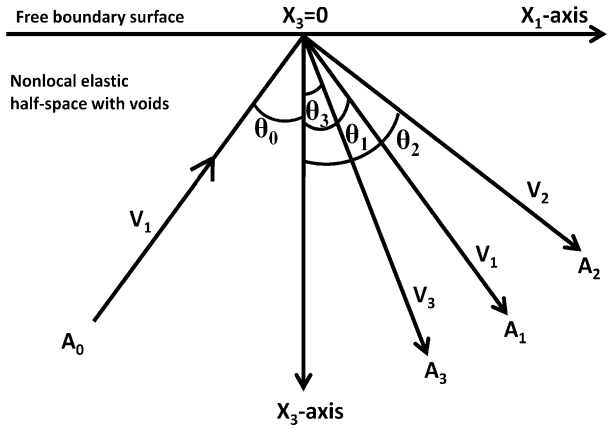
$$\zeta_i = \frac{(c_l^2 - c_i^2 - \epsilon^2 \omega^2) \rho \omega^2}{\beta c_i^2}. \tag{40}$$

### 4.1 Boundary Conditions

Since the boundary of the half-space  $M$  is mechanically stress free, therefore, the appropriate boundary conditions are the vanishing of force stress tensor and equilibrated stress tensor. Mathematically, these boundary conditions are written as: At  $x_3 = 0$

$$t_{33} = t_{31} = h_3 = 0, \tag{41}$$

Fig. 1 Geometry of the problem



or in terms of potentials as

$$\lambda(q_{,11} - U_{2,13}) + (\lambda + 2\mu)(q_{,33} + U_{2,13}) + \beta\phi = 0, \tag{42}$$

$$\mu(2q_{,13} + U_{2,11} - U_{2,33}) = 0, \tag{43}$$

$$\alpha\phi_{,3} = 0. \tag{44}$$

Inserting the potentials given by (36)–(38) into these boundary conditions, one can obtain a system of three non-homogeneous equations in three unknowns, which is written in matrix form as

$$[a_{ij}][X] = [B], \tag{45}$$

where  $[a_{ij}]$  is a  $3 \times 3$  matrix whose elements in non-dimensional form are given by

$$\begin{aligned} a_{11} &= 1, & a_{12} &= D^{-1} \left[ \lambda + (\lambda + 2\mu) \cot^2 \theta_2 - \frac{\beta \xi_2}{k_0^2} \right], \\ a_{13} &= 2\mu D^{-1} \cot \theta_3, & a_{21} &= 1, & a_{22} &= \frac{\cot \theta_2}{\cot \theta_0}, & a_{23} &= \frac{1 - \cot^2 \theta_3}{2 \cot \theta_0}, \\ a_{31} &= 1, & a_{32} &= \frac{\xi_2 \cot \theta_2}{\xi_1 \cot \theta_0}, & a_{33} &= 0, & D &= \lambda + (\lambda + 2\mu) \cot^2 \theta_0 - \frac{\beta \xi_1}{k_0^2}. \end{aligned}$$

$[X] = [X_1, X_2, X_3]^t$  is a column matrix, here ‘ $t$ ’ in the superscript represents the transpose of the matrix and

$$X_i = \frac{A_i}{A_0} \quad (i = 1, 2, 3)$$

are the reflection coefficients, and  $[B] = [-1, 1, 1]^t$ . The reflection coefficients  $X_i$  are obtained from (45) as

$$X_i = \frac{\Delta_i}{\Delta},$$

where  $\Delta$  is the determinant of the coefficient matrix  $[a_{ij}]$  and  $\Delta_i$  can be obtained in usual manner. Since the entries of the coefficient matrix are dependent on elastic properties of the

half-space, angle of incidence and frequency of the incident wave, hence all the reflection coefficients also depend on these parameters.

## 4.2 Particular Cases

### 4.2.1 Local Elastic Solid with Voids

If we neglect the nonlocality from the half-space, then we shall be left with an elastic material with voids only. For this purpose, setting the nonlocality parameter to zero, i.e.,  $\epsilon = 0$ , the coupling coefficients  $\zeta_i$ , ( $i = 1, 2$ ) reduce to

$$\zeta_i = \frac{(c_1^2 - c_i^2)\rho\omega^2}{\beta c_i^2}.$$

With these considerations, (45) will provide us the reflection coefficients in the corresponding problem. These expressions are similar as obtained earlier by Ciarletta and Sumbatyan [35].

### 4.2.2 Nonlocal Elastic Solid Without Voids

Here, we shall neglect the presence of voids from the half-space, but will account the presence of nonlocality. In this case, the third equation in (45) is automatically satisfied and the second equation yields  $A_2 = 0$ , indicating that the reflected wave propagating with phase speed  $V_2$  disappears and the reflected wave propagating with speed  $V_1$  is no more coupled. Thus, we shall be left with only two reflected waves, i.e., the reflected longitudinal displacement wave and reflected transverse wave. The remaining equations in (45) reduce to

$$[\bar{a}_{ij}][\bar{X}] = [\bar{B}], \quad (46)$$

where  $[\bar{a}_{ij}]$  is a  $2 \times 2$  matrix whose elements in non-dimensional form are given by

$$\bar{a}_{11} = \bar{a}_{21} = 1, \quad \bar{a}_{12} = \frac{2\mu \cot \theta_3}{[\lambda + (\lambda + 2\mu) \cot^2 \theta_0]}, \quad \bar{a}_{22} = \frac{1 - \cot^2 \theta_3}{2 \cot \theta_0},$$

$[\bar{X}] = [\bar{X}_1, \bar{X}_3]'$  is a column matrix, and  $[\bar{B}] = [-1, 1]'$ . We find that

$$\bar{X}_1 = \frac{-2\mu \cot \theta_3 \bar{X}_3}{[\lambda + (\lambda + 2\mu) \cot^2 \theta_0]} - 1,$$

$$\bar{X}_3 = \frac{4 \cot \theta_0 [\lambda + (\lambda + 2\mu) \cot^2 \theta_0]}{(1 - \cot^2 \theta_3) [\lambda + (\lambda + 2\mu) \cot^2 \theta_0] - 4\mu \cot \theta_0 \cot \theta_3}.$$

These are the reflection coefficients due to incidence of longitudinal displacement wave in the present case. It can be seen that these coefficients are functions of material parameters, non-locality parameter, frequency as well as angle of incidence of the incident wave.

### 4.2.3 Classical Elastic Solid

If we neglect the presence of nonlocality and voids simultaneously from the half-space, then we shall be left with the reflection problem of incident longitudinal displacement wave from

the boundary surface of classical elastic half-space. Setting the parameters corresponding to nonlocality and voids equal to zero, one can see that the last equation in the matrix equation (45), corresponding to vanishing of equilibrated stress is identically satisfied. This means that the reflected wave corresponding to change in void volume fraction disappears. With  $A_2 = 0$ , the remaining two boundary conditions reduce to (2)–(10) given in Ewing et al. [36] for the corresponding problem, for which we need to take  $\lambda = \mu$  and the change of angle of incidence into angle of emergence will be required.

*Remark* One can observe that the expressions of reflection coefficients obtained in Sect. 4.2.2 for the case of nonlocal elastic solid without voids are same as those obtained in Sect. 4.2.3 in the case of classical elastic solid. Note that in the earlier case, the speeds of waves are dispersive (as discussed in Sect. 3.2.3, while in the classical case, the speeds of waves are non-dispersive. Thus, the reflection coefficients do not depend upon the frequency in classical elastic case, while they depend on frequency too in case of nonlocal elastic solid without voids.

### 5 Energy Partitioning

In order to physically justify the analytic expressions of the reflection coefficients in the problem, we must verify the energy balance at the boundary surface. To discuss the partitioning of incident energy at the boundary surface, the rate of energy transmission  $P$  per unit area is given by (see Achenbach [37])

$$P = t_{33}^L \dot{u}_3 + t_{31}^L \dot{u}_1 + h_3^L \dot{\phi}. \tag{47}$$

Let  $\langle P_0 \rangle$  denotes the average energy carried along incident wave,  $\langle P_i \rangle$  ( $i = 1, 2$ ) denote the average energy carried along reflected coupled longitudinal waves and  $\langle P_3 \rangle$  denotes the average energy carried along reflected transverse wave. Using (11), (12), (22) and (35) in (47), we get the following expressions

$$\langle P_0 \rangle = \frac{1}{2} k_0^4 v \cot \theta_0 \left( D + 2\mu - \frac{\alpha \zeta_1^2}{k_0^2} \right) A_0^2, \tag{48}$$

$$\langle P_1 \rangle = -\frac{1}{2} k_0^4 v \cot \theta_1 \left[ \lambda + (\lambda + 2\mu) \cot^2 \theta_1 - \frac{\beta \zeta_1}{k_0^2} + 2\mu - \frac{\alpha \zeta_1^2}{k_0^2} \right] A_1^2, \tag{49}$$

$$\langle P_2 \rangle = -\frac{1}{2} k_0^4 v \cot \theta_2 \left[ \lambda + (\lambda + 2\mu) \cot^2 \theta_2 - \frac{\beta \zeta_2}{k_0^2} + 2\mu - \frac{\alpha \zeta_2^2}{k_0^2} \right] A_2^2, \tag{50}$$

$$\langle P_3 \rangle = -\frac{1}{2} k_0^4 v \mu \cot \theta_3 (1 + \cot^2 \theta_3) A_3^2. \tag{51}$$

We define energy ratio  $E_i$  ( $i = 1, 2, 3$ ) corresponding to the  $i$ th reflected wave at  $x_3 = 0$  as the ratio of energy carried along  $i$ th reflected wave to the energy carried along the incident wave, given by

$$E_i = \frac{\langle P_i \rangle}{\langle P_0 \rangle}. \tag{52}$$

Thus, for an incident set of coupled longitudinal wave having phase speed  $V_1$ , the energy ratios of reflected waves are given by

$$E_1 = -X_1^2, \tag{53}$$

$$E_2 = - \frac{[\lambda + (\lambda + 2\mu) \cot^2 \theta_2 - \frac{\beta \xi_2}{k_0^2} + 2\mu - \frac{\alpha \xi_2^2}{k_0^2}] \cot \theta_2}{(D + 2\mu - \frac{\alpha \xi_1^2}{k_0^2}) \cot \theta_0} X_2^2, \tag{54}$$

$$E_3 = - \frac{\mu \cot \theta_3 (1 + \cot^2 \theta_3)}{(D + 2\mu - \frac{\alpha \xi_1^2}{k_0^2}) \cot \theta_0} X_3^2, \tag{55}$$

where  $D$  has been defined earlier. We note that these energy ratios also depend on the elastic properties of the medium, angle of incidence and amplitude ratios.

### 6 Numerical Results and Discussion

In order to study the characteristics of wave propagation through nonlocal elastic material with voids, we have computed their phase speeds and corresponding attenuation coefficients for a specific model. The amplitude and energy ratios corresponding to reflected waves due to incidence of a set of coupled longitudinal waves at the free surface of the half-space  $M$ , have also been computed and discussed. For the purpose of numerical computations, we have borrowed the values of relevant material parameters from Puri and Cowin [22] and Eringen [33]. These are given in Table 1.

The phase speeds and corresponding attenuation coefficients of existed waves have been computed from the formulae (33) and (34).

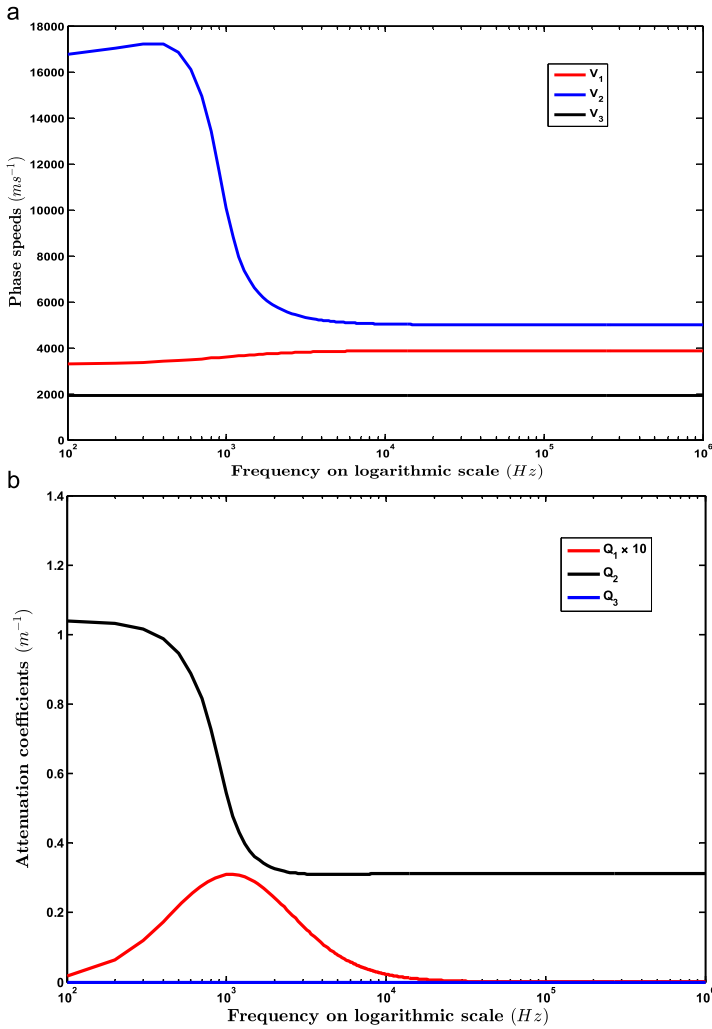
Figure 2a depicts the variation of phase speeds  $V_i$  ( $i = 1, 2, 3$ ) with the frequency  $f$  in the range  $10^2 < f < 10^6$  Hz on logarithmic scale where  $f$  is given by the relation  $\omega = 2\pi f$ . It can be noticed that all the waves are dispersive. The wave with speed  $V_2$  is highly dispersive in the certain initial range of frequency  $f$  than the other two waves. The wave with phase speed  $V_2$  first increases slightly from certain value with increase in frequency, then it starts decreasing rapidly with frequency in the range  $400 < f < 5000$  Hz approximately, after that it becomes almost constant. On comparing the magnitudes of phase speeds of these waves, we see that  $0 < V_3 < V_1 < V_2$  showing that the wave with speed  $V_2$  is the fastest one and the wave with speed  $V_3$  is the slowest one. This conclusion is in concurrence with those obtained by Puri and Cowin [22]. Moreover, the wave with speed  $V_2$  is weakly dispersive beyond the range  $400 < f < 5000$  Hz approximately, while the wave with speed  $V_3$  is weakly dispersive throughout the frequency range chosen. The wave with speed  $V_1$  is relatively more dispersive than the wave with speed  $V_3$ . The wave with speed  $V_3$  is weakly dispersive throughout the range due to very small value of the term  $\epsilon^2 \omega^2$  (occurring in the expression of its speed) chosen in the model.

Figure 2b depicts the variation of attenuation coefficients  $Q_i$  ( $i = 1, 2, 3$ ) with the frequency  $f$  for the existing waves. It is clear from the figure that the attenuation coefficient

**Table 1** Numerical values of parameters

Symbol	Value	Symbol	Value
$\lambda$	$1.5 \times 10^{10}$ Pa	$\mu$	$7.5 \times 10^9$ Pa
$\xi$	$1.2 \times 10^{10}$ Pa	$\beta$	$1 \times 10^{10}$ Pa
$\alpha$	$8 \times 10^9$ Pa m <sup>2</sup>	$\tau$	$1 \times 10^6$ Pa s
$\rho$	$2 \times 10^3$ kg/m <sup>3</sup>	$e_0$	0.39
$a$	$0.5 \times 10^{-9}$ m	$\chi$	$0.16$ m <sup>2</sup>





**Fig. 2** a Variation of  $V_i$  ( $i = 1, 2, 3$ ) with respect to frequency. b Variation of  $Q_i$  ( $i = 1, 2, 3$ ) with respect to frequency

$Q_2$  corresponding to the wave with phase speed  $V_2$  dominates heavily over the attenuation coefficients of other waves. The attenuation coefficient  $Q_3$  is zero in the considered frequency range, indicating that the corresponding wave is non-attenuating. The attenuation coefficient  $Q_1$  too is very very small and it has been shown in figure, after magnifying by a factor of 10. It is also observed that the coefficients  $Q_1$  and  $Q_2$  are frequency dependent in low frequency range  $10^2 < f < 10^4$ , and after that the coefficient  $Q_2$  is almost constant, while  $Q_1$  is almost zero.

Figure 3a depicts the comparison between the phase speeds of the coupled longitudinal waves ( $V_1$  and  $V_2$ ) with the speed of classical longitudinal wave ( $c_l$ ). It is observed that the phase speed  $V_1$  and  $c_l$  are almost same only in the high frequency range, however in low frequency range  $V_1$  is less than  $c_l$ . The phase speed  $V_2$  is found to be always higher than  $c_l$

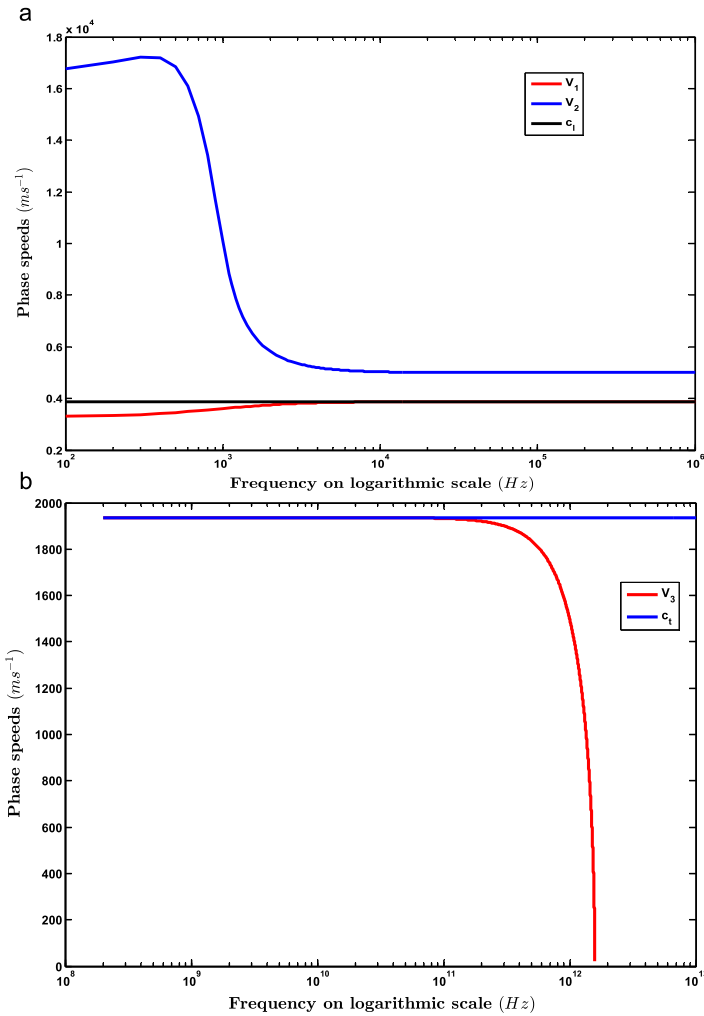


**Fig. 3** a Comparison of  $V_i$  ( $i = 1, 2$ ) with  $c_l$ . b Comparison of  $V_3$  with  $c_l$

for all frequencies chosen, but the difference is more prominent in the low frequency range where the wave is highly dispersive.

Figure 3b shows a comparison of phase speed of transverse wave  $V_3$  with classical shear wave  $c_l$ . First, we note that the wave with speed  $V_3$  is dispersive, while the classical shear wave is non-dispersive. The figure indicates that the wave with speed  $V_3$  almost travels with the speed of classical shear wave in the initial range of frequency, but for very-very high frequency range the wave with speed  $V_3$  approaches to zero rapidly, while classical shear wave maintains its value as was expected. This is not surprising at all, because the speed  $c_3$  of shear wave given by formula (31) vanishes at  $\omega = c_l/\epsilon$ . Beyond  $\omega = c_l/\epsilon$ , it becomes purely imaginary indicating that the wave is no more a progressive wave.

To investigate the effect of nonlocality parameter on existing waves, we define a non-dimensional nonlocality parameter  $\bar{\epsilon}$  as:  $\bar{\epsilon} = \epsilon^2 \omega_0^2 / c_l^2$ , where  $\omega_0$  is a standard angular frequency. By taking  $\omega_0 = 2\pi \times 2000$   $s^{-1}$ , Fig. 4 depicts the effect of  $\bar{\epsilon}$  ( $0.1 \times 10^{-5}$  to

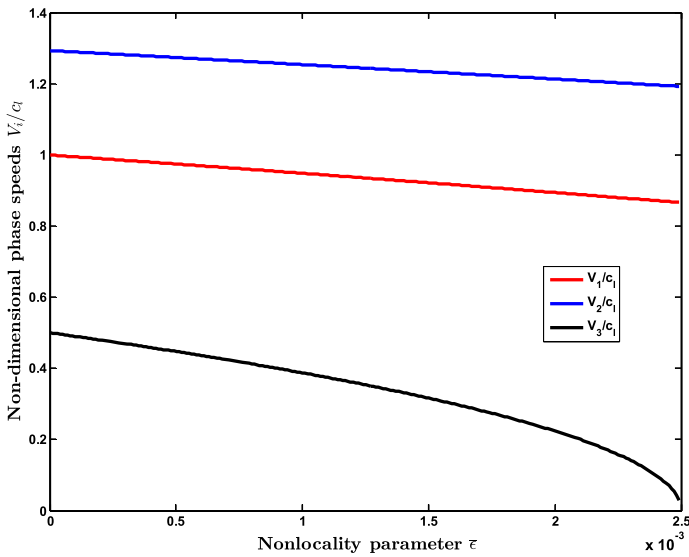


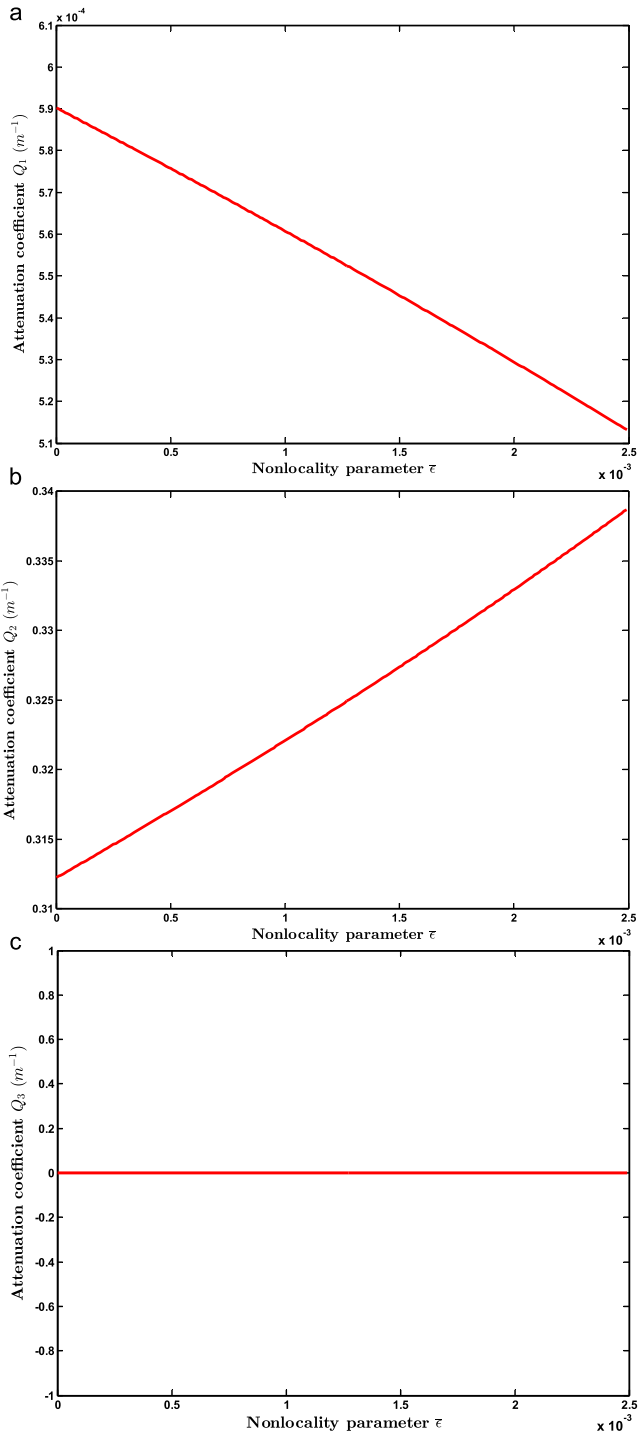
**Fig. 4** Variation of  $V_i/c_l$  ( $i = 1, 2, 3$ ) with respect to  $\bar{\epsilon}$

$2.5 \times 10^{-3}$  at frequency  $f = 20$  kHz) on the phase speeds of existing waves. It can be noticed that the transverse wave is highly influenced by the nonlocality parameter than the coupled longitudinal waves. The effect of  $\bar{\epsilon}$  on coupled longitudinal waves is similar in nature and linearly decreasing. The effect of nonlocality on the corresponding attenuation coefficients has been depicted through Figs. 5a–c. It is clear from these figures that the attenuation coefficient of transverse wave is zero as was expected before hand, while the attenuation coefficients of other waves are non-zero and possess opposite behavior against  $\bar{\epsilon}$ .

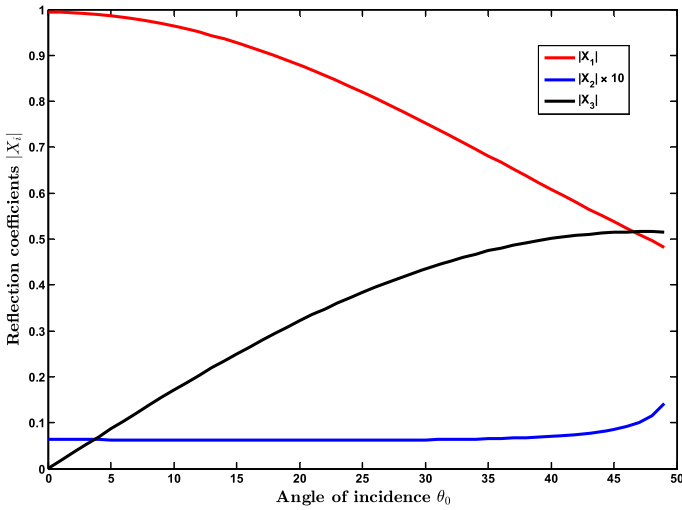
Figure 6 depicts the variation of absolute values of reflection coefficients  $X_i$  ( $i = 1, 2, 3$ ) with the angle of incidence  $\theta_0$  of a set of coupled longitudinal waves having phase speed  $V_1$  for the range  $0 < \theta_0 < 50^\circ$  at a fixed frequency  $f = 20$  kHz. The angle  $\theta_0 = 50^\circ$  is found to be a critical angle, beyond which total reflection occurs. This is because the phase speed  $V_2$  is higher than  $V_1$ , and therefore Snell’s law ensures the occurrence of total reflection for  $\theta_0 > 50^\circ$ . From the figure, it is observed that the reflection coefficient  $X_1$  has its maximum value equal to unity at normal incidence, its value then decreases with increase of angle of incidence  $\theta_0$ . The reflection coefficient  $X_2$  is found to be very small, so it has been shown after magnifying by a factor of 10. It is observed that the absolute value of reflection coefficient  $X_2$  is almost constant over the entire range of  $\theta_0$ , while the reflection coefficient  $X_3$  is zero at normal incidence and it increases with increase of angle of incidence  $\theta_0$ .

Figure 7 depicts the variation of absolute values of corresponding energy ratios  $E_i$  ( $i = 1, 2, 3$ ) with the angle of incidence  $\theta_0$ . We see that the behavior of energy ratios with angle of incidence is similar to the behavior of corresponding amplitude ratios. This is quite appealing as the energy ratios are proportional to the square of corresponding amplitude ratios at each angle of incidence. It has been noticed that the sum of real parts of energy ratios  $E_i$  ( $i = 1, 2, 3$ ) is unity, while the sum of corresponding imaginary parts of energy ratios  $E_i$  ( $i = 1, 2, 3$ ) is zero at each angle of incidence.

Figures 8a–c depict the variation of absolute values of reflection coefficients with the non-dimensional nonlocality parameter  $\bar{\epsilon}$  (ranging from  $0.1 \times 10^{-5}$  to  $2.5 \times 10^{-3}$  at frequency  $f = 20$  kHz and angle of incidence  $\theta_0 = 15^\circ$ ). We have observed that the value of



**Fig. 5** a Variation of  $Q_1$  with respect to  $\bar{\tau}$ . b Variation of  $Q_2$  with respect to  $\bar{\tau}$ . c Variation of  $Q_3$  with respect to  $\bar{\tau}$



**Fig. 6** Variation of  $|X_i|$  ( $i = 1, 2, 3$ ) with respect to  $\theta_0$

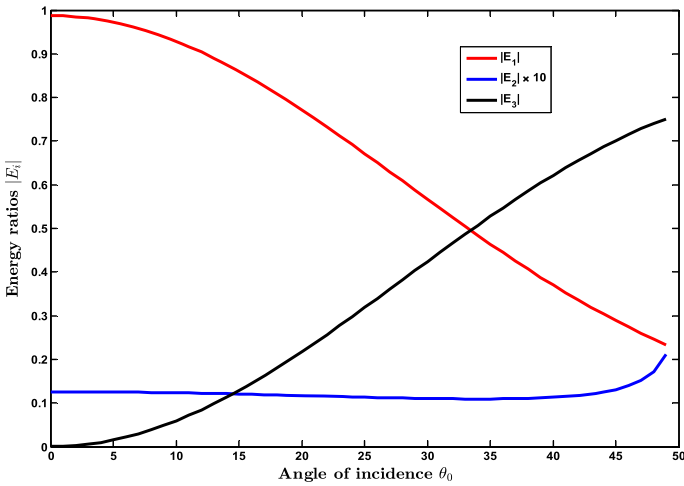


**Fig. 7** Variation of  $|E_i|$  ( $i = 1, 2, 3$ ) with respect to  $\theta_0$

$X_1$  increases with  $\bar{\epsilon}$ , but with very small rate. The value of amplitude ratio  $X_2$  decreases with  $\bar{\epsilon}$  but the rate of decrease is again very small. The value of amplitude ratio  $X_3$  is almost constant in the entire range of  $\bar{\epsilon}$ , though it appears as increasing but not appreciable. We have also verified that for different values of nonlocality parameter  $\bar{\epsilon}$ , the energy balance law is satisfied at fixed angle of incidence.

Figure 9a depicts the variation of absolute values of coupling coefficients  $\zeta_1$  and  $\zeta_2$  defined in (40) with the frequency  $f$  in the range  $10^2 < f < 10^6$  Hz on logarithmic scale. We found that  $\zeta_1$  is very small as compared to  $\zeta_2$ , therefore we have plotted  $\zeta_1$  after magnifying by a factor of  $10^6$ . We observe that  $\zeta_2$  increases monotonically with increase of frequency.

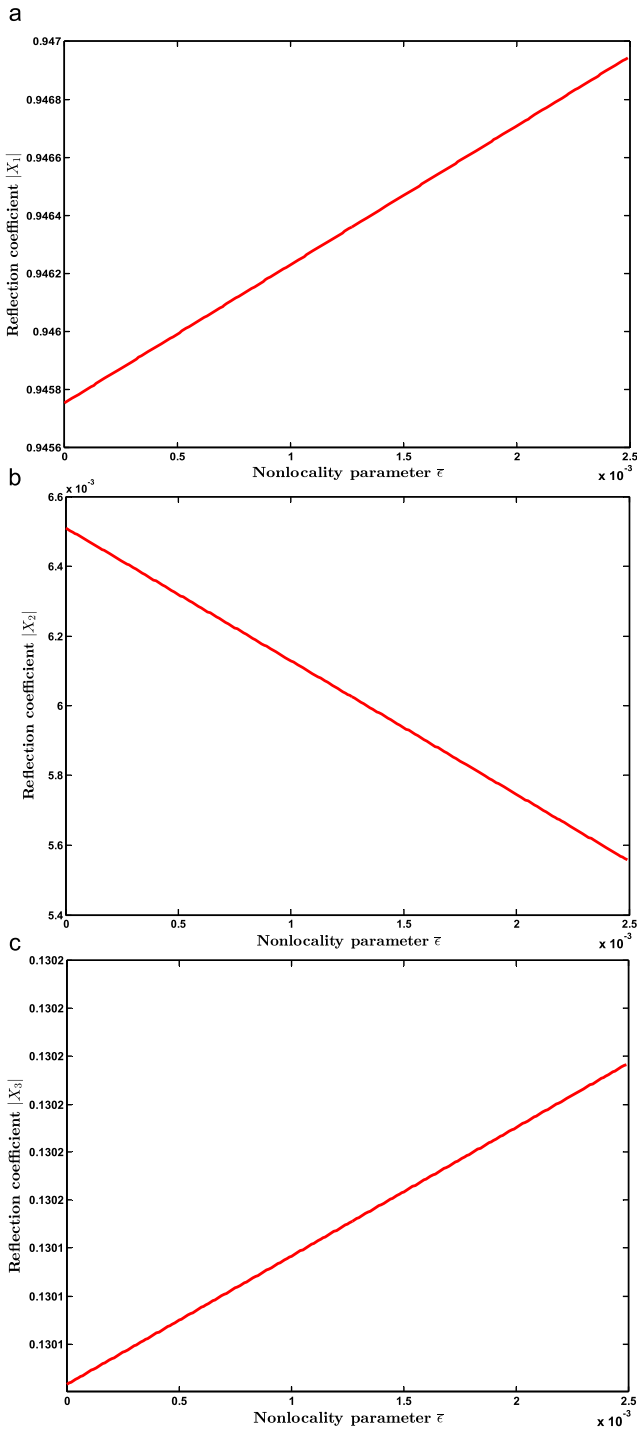


**Fig. 8** a Variation of  $|X_1|$  with respect to  $\bar{\epsilon}$ . b Variation of  $|X_2|$  with respect to  $\bar{\epsilon}$ . c Variation of  $|X_3|$  with respect to  $\bar{\epsilon}$

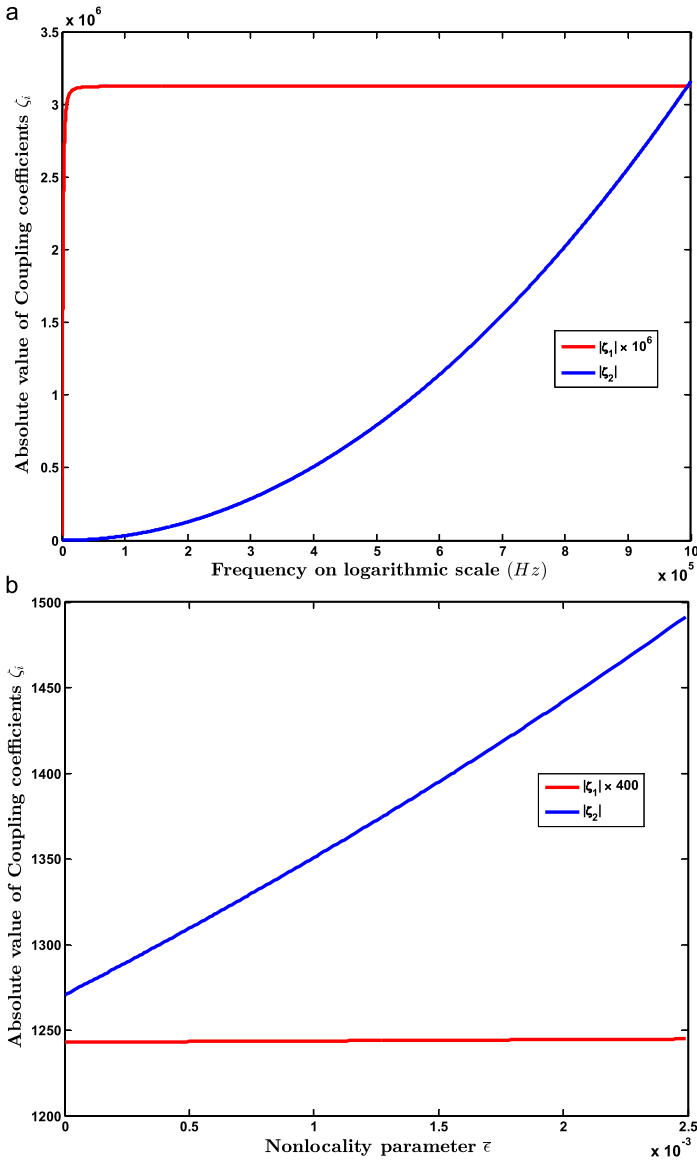


**Fig. 9** **a** Variation of  $|\zeta_1|$  and  $|\zeta_2|$  with respect to frequency. **b** Variation of  $|\zeta_1|$  and  $|\zeta_2|$  with respect to  $\bar{\tau}$

Figure 9b depicts the variation of absolute values of coupling coefficients with the non-dimensional nonlocality parameter  $\bar{\tau}$  (ranging from  $0.1 \times 10^{-5}$  to  $2.5 \times 10^{-3}$  at frequency  $f = 20$  kHz). It is observed that  $\zeta_1$  remains almost constant, while  $\zeta_2$  increases almost linearly with  $\bar{\tau}$ . Since the value of  $\zeta_1$  is very small, therefore its plot has been depicted after magnifying by a factor of 400.

Figure 10 depicts the variation of absolute values of  $c_i$  ( $i = 1, 2, 3$ ) against low frequency ranging from 0– $10^6$  Hz on logarithmic scale. It can be seen that the absolute value  $c_3$  is constant as was expected since the contribution of the term  $\epsilon^2 \omega^2$  in (31) is almost neg-

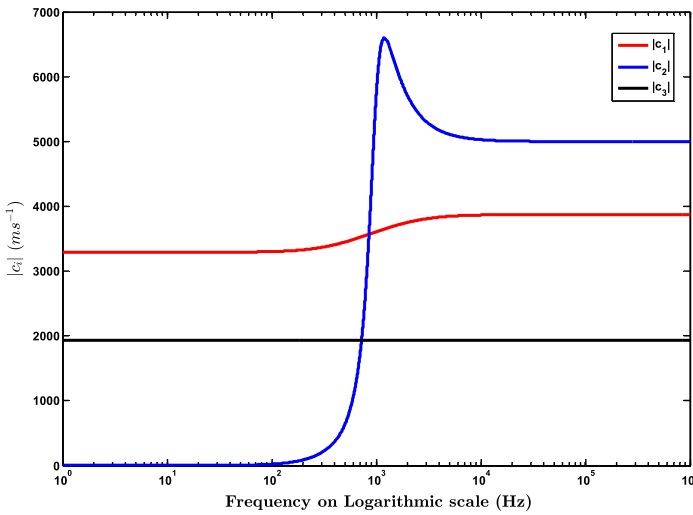
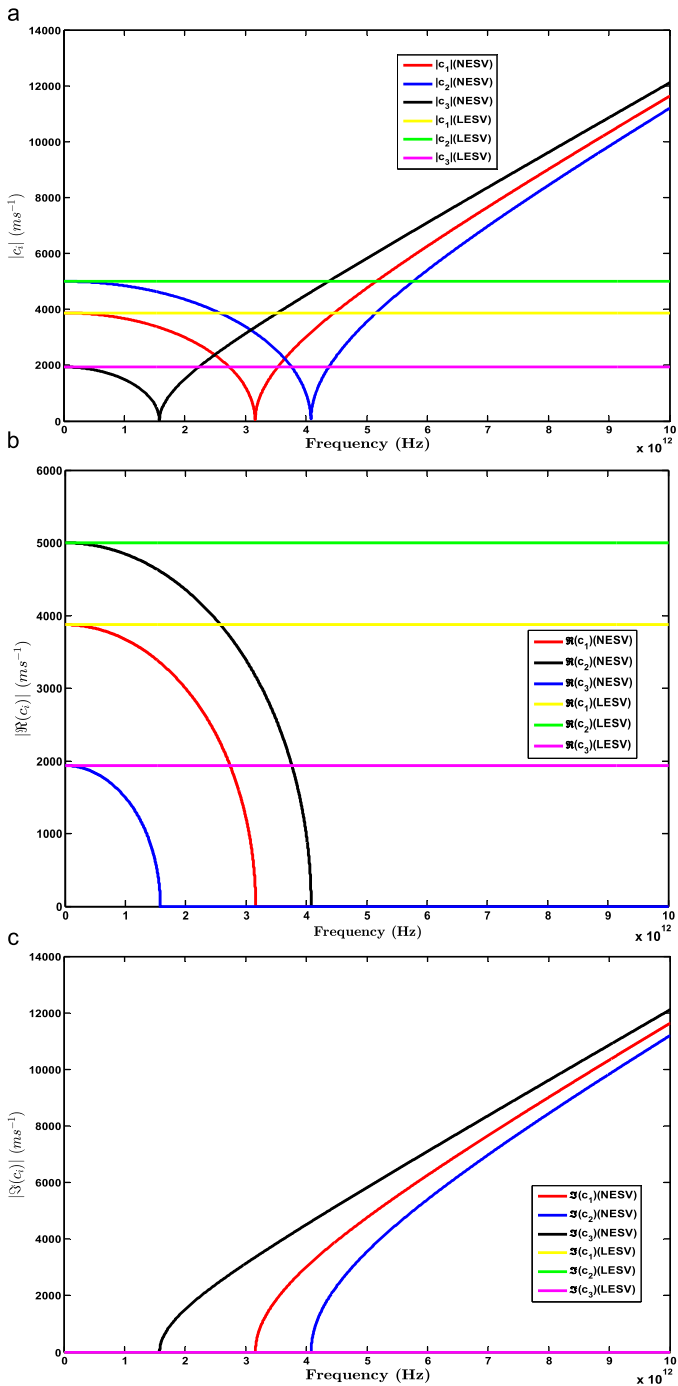


**Fig. 10** Variation of  $|c_i|$  ( $i = 1, 2, 3$ ) with respect to frequency

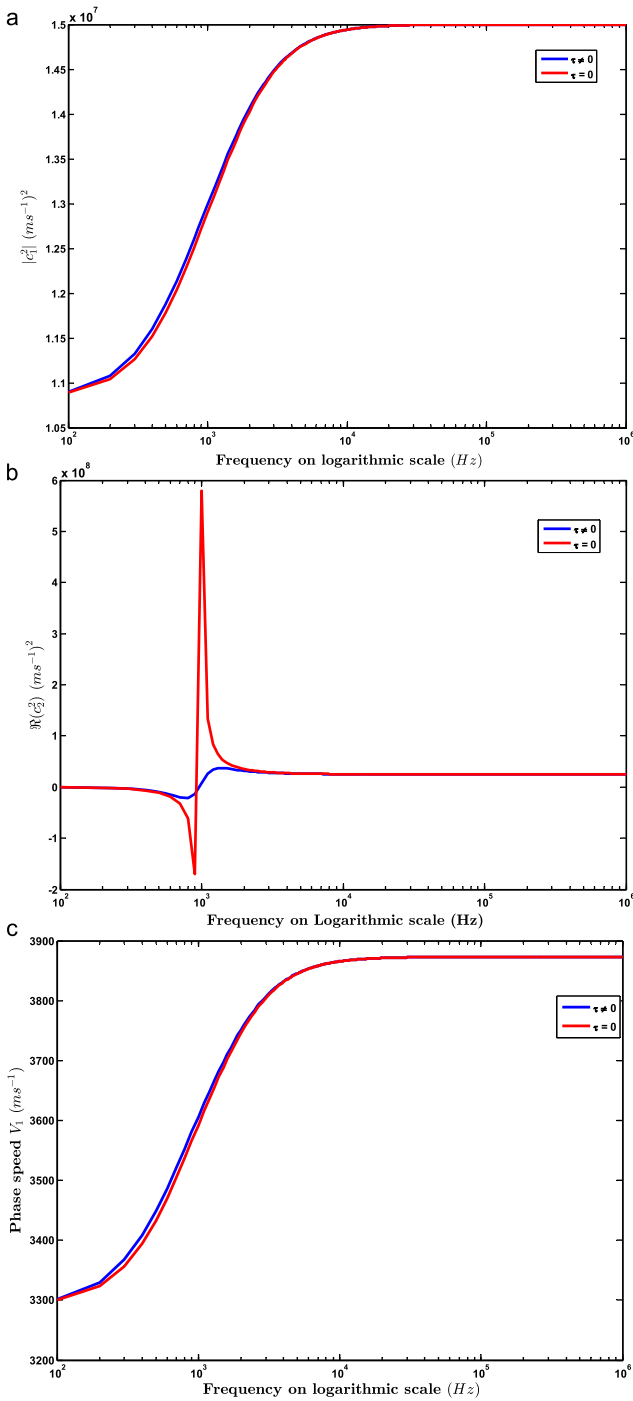
ligible for low frequency range. The absolute value of  $c_1$  depends significantly on frequency only for very low frequency. The absolute value of  $c_1$  starts from some definite value at zero frequency, it increases very slowly with increase of frequency and finally goes around  $3.9 \text{ km s}^{-1}$  with further increase of frequency parameter. The dependence of absolute value of  $c_2$  on frequency is interesting. First, we note that as  $\omega$  approaches to zero, the value of  $c_2$  also approaches to zero, which is supporting our inference discussed in Sect. 3.1. As  $\omega$  takes value greater than  $10^2 \text{ Hz}$ , the absolute value of  $c_2$  increases very fast and attains maximum value around  $6.6 \text{ km s}^{-1}$  at  $\omega = 2.4\pi \text{ kHz}$  and then starts decreasing with further increase of  $\omega$  and soon becomes almost constant keeping its value around  $5 \text{ km s}^{-1}$ .

Figure 11a depicts the variation of absolute values of  $c_i$  ( $i = 1, 2, 3$ ) against frequency parameter ranging from  $10^8$ – $10^{13} \text{ Hz}$  for both local as well as nonlocal elastic material with voids. It is very much clear from this figure that the waves are dispersive/non-dispersive in nonlocal/local elastic material with voids (NESV/LESV). We further notice that the speed of each propagating wave vanishes at certain value of frequency parameter  $f_{c_i}$  in nonlocal elastic material with voids. These specific values of frequency may be declared as critical frequencies for the respective waves. This is because at these critical values of frequency, the respective waves change their behavior dramatically. What is happening there can be made clear through Figs. 11b and c. From Figs. 11b and c, we see that beyond the range  $0 < f < f_{c_i}$ , the real parts of all the propagating waves are almost zero in nonlocal elastic solid with voids but they maintain their constant value in the case of local elastic solid with voids. This means that after their critical frequencies in NESV, the speeds of all the waves are purely imaginary indicating that these waves are no more propagating waves but they just represent the distance decaying vibrations. The imaginary part of speed  $c_3$  is zero within the range indicating that it is non-attenuating propagating wave as has been clarified earlier in Sect. 3. The waves propagating with speeds  $c_1$  and  $c_2$  are poorly attenuating as the imaginary parts of their speeds is very-very small within the range. However, the wave with speed  $c_1$  is relatively poorer than  $c_2$  in attenuation. This attenuation is clearly arising due to the presence of voids in the medium, in the absence of which the wave with speed  $c_2$  disappears and the wave with speed  $c_1$  propagates with real speed for range  $0 < \omega < c_1/\epsilon$ .



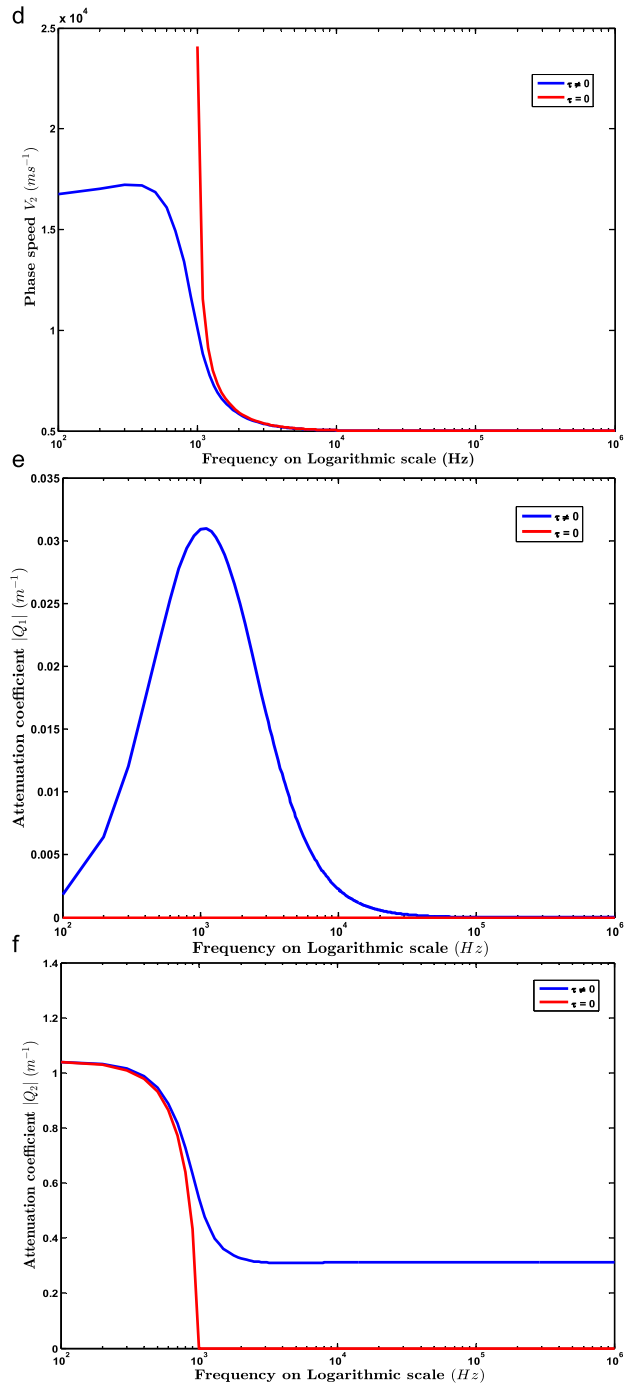


**Fig. 11** **a** Variation of  $|c_i|$  ( $i = 1, 2, 3$ ) with respect to frequency and its comparison in nonlocal and local elastic solid with voids. **b** Variation of  $|\Re(c_i)|$  ( $i = 1, 2, 3$ ) with respect to frequency and its comparison in nonlocal and local elastic solid with voids. **c** Variation of  $|\Im(c_i)|$  ( $i = 1, 2, 3$ ) with respect to frequency and its comparison in nonlocal and local elastic solid with voids



**Fig. 12** **a** Comparison of  $|c_1^2|$  in voigt and non-voigt solid. **b** Comparison of  $\Re(c_2^2)$  in voigt and non-voigt solid. **c** Comparison of  $V_1$  in voigt and non-voigt solid. **d** Comparison of  $V_2$  in voigt and non-voigt solid. **e** Comparison of  $|Q_1|$  in voigt and non-voigt solid. **f** Comparison of  $|Q_2|$  in voigt and non-voigt solid

Fig. 12 (continued)



Figures 12a–f show the comparison of  $c_1^2$ ,  $c_2^2$ , phase speeds  $V_1$ ,  $V_2$ , the attenuation coefficients  $Q_1$  and  $Q_2$  for voigt ( $\tau \neq 0$ ) and non-voigt ( $\tau = 0$ ) elastic solid with voids in low frequency range on logarithmic scale. From Fig. 12a, we observe that for  $\tau = 0$ , the absolute value of  $c_1^2$  is little smaller than that of for  $\tau \neq 0$  showing that the effect of  $\tau$  on  $c_1^2$  is not much appreciable in the chosen frequency range. Next, we have seen that  $c_2^2$  is real when  $\tau = 0$  and complex when  $\tau \neq 0$ . In Fig. 12b, we have plotted the graphs of  $\Re(c_2^2)$  with frequency for voigt and non-voigt cases. From this figure, we note that the wave traveling with speed  $c_2$  faces a cut-off frequency for non-voigt ( $\tau = 0$ ) case only. This shows that  $\tau$  has significant impact on the propagation of this wave. It has been found that the value of cut-off frequency is exactly at  $\omega = \sqrt{\xi/\rho\chi}$  as has been mentioned in Sect. 3.2.1. For  $\tau = 0$ , the  $c_2^2$  has a point of infinite discontinuity at  $\omega_c (= \sqrt{\xi/\rho\chi})$  below  $\omega_c$ ,  $c_2^2 < 0$  and beyond  $\omega_c$ ,  $c_2^2 > 0$ , while for  $\tau \neq 0$ ,  $c_2^2$  does not face any such point of infinite discontinuity. This is because the quantity  $A$  occurring in the denominator of  $c_2^2$  remains complex. Thus, we can conclude that for the non-voigt case, the wave with speed  $c_2$  is a propagating wave only for  $\omega > \omega_c$ . Figures 12c and d show the comparison of the phase speeds  $V_1$  and  $V_2$  respectively for voigt and non-voigt cases. Very minute effect of  $\tau$  has been observed on  $V_1$ , while  $V_2$  does not exist for  $\omega < \omega_c$ . This is quite clear because  $c_2^2 < 0$  for  $\omega < \omega_c$ , hence  $\Re(c_2) = 0$  and does not allow the phase speed  $V_2$  to exist in the said range. For non-voigt elastic solid with voids, the speed  $c_2^2$  remains complex and hence  $\Re(c_2)$  does not vanish, which in turn allows the  $V_2$  to exist for all frequencies in the said range. Figures 12e and f show the comparison of corresponding attenuation coefficients. We observe that the attenuation coefficient  $Q_1$  is zero in the case when  $\tau = 0$ , while it has significant value in the other case. Figure 12f shows that the absolute value of the attenuation coefficient  $Q_2$  is zero after cut-off frequency in the case when  $\tau = 0$ , but in the other case, it achieve significant constant value. This is obviously acceptable as the value of  $c_2$  is real and positive for  $\omega > \omega_c$  in case of  $\tau = 0$ . It has also been observed that the behavior of voigt and non-voigt solids is almost same in higher frequency range.

## 7 Conclusions

In this paper, we have extended the concept of nonlocality to the theory of elastic material with voids. The constitutive relations and governing equations are developed for linear isotropic nonlocal elastic solid with voids. The possibility of plane wave propagation has been explored and the reflection phenomenon of a plane wave striking obliquely at the stress free boundary surface of a nonlocal elastic half-space with voids has also been investigated. We conclude that

- (i) Three waves propagating with distinct speeds may travel in a nonlocal elastic solid with voids, consisting of two sets of coupled longitudinal waves and an independent transverse wave. The coupled waves are found to be dispersive and attenuating in nature, while the transverse wave is dispersive but non-attenuating in low frequency range. All the waves are found to be influenced by the nonlocality of the medium.
- (ii) The waves propagating with phase speeds  $V_1$  and  $V_2$  are influenced by the void parameters, but the wave propagating with phase speed  $V_3$  is independent of the void parameters.
- (iii) Transverse wave propagating with speed  $c_3$  faces a critical frequency  $\omega_{c_3}$ , above which the wave is no more a propagating wave. While the coupled waves propagating with speeds  $c_i$  ( $i = 1, 2$ ) may face critical frequencies provided  $\Re(c_i) = 0$  at  $\omega = \omega_{c_i}$  ( $i = 1, 2$ ). For  $\omega > \omega_{c_i}$ , the corresponding waves will no more be propagating waves.

- (iv) In the low frequency range, for the wave traveling with speed  $c_2$  through non-voigt elastic solid with voids, there exist a cut-off frequency in contrast to the case of voigt elastic solid with voids.
- (v) The wave propagating with phase speed  $V_3$  is highly influenced by the nonlocality parameter as compared to coupled waves.
- (vi) In the reflection problem, the maximum amount of incident energy is carried along the reflected coupled longitudinal waves, which is of the same speed as that of the incident coupled waves. The reflection coefficients and corresponding energy ratios depend upon the nonlocality parameter, void parameters, angle of incidence and the frequency of the incident wave.
- (vii) The reflection coefficient corresponding to the reflected wave propagating with phase speed  $V_1$  increases with the nonlocality parameter, while the reflection coefficient corresponding to wave propagating with phase speed  $V_2$  decreases and the reflection coefficient corresponding to wave propagating with phase speed  $V_3$  remains almost constant at fixed frequency.
- (viii) One of the coupling coefficients ( $\zeta_2$ ) is highly dependent on the frequency and the nonlocality parameters. It increases almost linearly with the nonlocality parameter.

**Acknowledgements** One of the authors (GK) acknowledges the financial support provided by Council of Scientific and Industrial Research, New Delhi, INDIA, in the form of JRF through Grant No. 09/135(0715)/2015-EMR-1. Authors are grateful to the unknown reviewers for their constructive comments, which had led to an improvement on the manuscript.

## References

1. Altan, B.S.: Uniqueness in the linear theory of nonlocal elasticity. *Bull. Tech. Univ. Istanbul* **37**, 373–385 (1984)
2. Chirita, S.: On some boundary value problems in nonlocal elasticity. In: *Amale Stiintifice ale Universitatii "AL. I. CUZA" din Iasi Tomul*, vol. xxii, p. 2 (1976)
3. Craciun, B.: On nonlocal thermoelasticity. *Ann. St. Univ., Ovidius Constanta* **5**(1), 29–36 (1996)
4. Edelen, D.G.B., Laws, N.: On the thermodynamics of systems with nonlocality. *Arch. Ration. Mech. Anal.* **43**(1), 24–35 (1971)
5. Edelen, D.G.B., Green, A.E., Laws, N.: Nonlocal continuum mechanics. *Arch. Ration. Mech. Anal.* **43**(1), 36–44 (1971)
6. Eringen, A.C., Edelen, D.G.B.: On nonlocal elasticity. *Int. J. Eng. Sci.* **10**(3), 233–248 (1972)
7. Eringen, A.C.: Nonlocal polar elastic continua. *Int. J. Eng. Sci.* **10**(1), 1–16 (1972)
8. Eringen, A.C.: On nonlocal fluid mechanics. *Int. J. Eng. Sci.* **10**(6), 561–575 (1972)
9. Eringen, A.C.: Nonlocal continuum theory of liquid crystals. *Mol. Cryst. Liq. Cryst.* **75**(1), 321–343 (1981)
10. Eringen, A.C.: Memory dependent nonlocal electrodynamics. In: Hsieh, R.K.T. (ed.) *Mechanical Modelling of New Electromagnetic Materials. Proceedings of IUTAM Symposium*, pp. 45–49 (1990)
11. Eringen, A.C.: Memory-dependent nonlocal electromagnetic elastic solids and superconductivity. *J. Math. Phys.* **32**(3), 787–796 (1991)
12. McCay, B.M., Narsimhan, M.L.N.: Theory of nonlocal electromagnetic fluids. *Arch. Mech.* **33**(3), 365–384 (1981)
13. Narsimhan, M.L.N., McCay, B.M.: Dispersion of surface waves in nonlocal dielectric fluids. *Arch. Mech.* **33**, 385–400 (1981)
14. Khurana, A., Tomar, S.K.: Wave propagation in nonlocal microstretch solid. *Appl. Math. Model.* **40**(11–12), 5858–5875 (2016)
15. Narendar, S.: Spectral finite element and nonlocal continuum mechanics based formulation for torsional wave propagation in nanorods. *Finite Elem. Anal. Des.* **62**, 65–75 (2012)
16. Narendar, S., Gopalakrishnan, S.: Ultrasonic wave characteristics of nanorods via nonlocal strain gradient models. *J. Appl. Phys.* **107**(8), 084312 (2010)
17. Narendar, S., Gopalakrishnan, S.: Nonlocal scale effects of ultrasonic wave characteristics of nanorods. *Physica E* **42**(5), 1601–1604 (2010)

18. Narendar, S., Mahapatra, Roy, D., Gopalakrishnan, S.: Prediction of nonlocal scaling parameter for armchair and zigzag single-walled carbon nanotubes based on molecular structural mechanics, nonlocal elasticity and wave propagation. *Int. J. Eng. Sci.* **49**(6), 509–522 (2011)
19. Malagu, M., Benvenuti, E., Simone, A.: One-dimensional nonlocal elasticity for tensile single-walled carbon nanotubes: a molecular structural mechanics characterization. *Eur. J. Mech. A, Solids* **54**, 160–170 (2015)
20. Nunziato, J.W., Cowin, S.C.: A non linear theory of elastic materials with voids. *Arch. Ration. Mech. Anal.* **72**, 175–201 (1979)
21. Cowin, S.C., Nunziato, J.W.: Linear elastic materials with voids. *J. Elast.* **13**, 125–147 (1983)
22. Puri, P., Cowin, S.C.: Plane waves in linear elastic materials with voids. *J. Elast.* **15**, 167–183 (1985)
23. Iesan, D.: A theory of thermoelastic material with voids. *Acta Mech.* **60**(1), 67–89 (1986)
24. Singh, J., Tomar, S.K.: Planes wave in thermo-elastic material with voids. *Mech. Mater.* **39**, 932–940 (2007)
25. Iesan, D.: On the theory of viscoelastic mixtures. *J. Therm. Stresses* **27**(12), 1125–1148 (2004)
26. Tomar, S.K., Bhagwan, J., Steeb, H.: Time harmonic waves in a thermoviscoelastic material with voids. *J. Vib. Control* **20**(8), 1119–1136 (2014)
27. Sharma, K., Kumar, P.: Propagation of plane waves and fundamental solution in thermoviscoelastic medium with voids. *J. Therm. Stresses* **36**(2), 94–111 (2013)
28. D'Apice, C., Chirita, S.: Plane harmonic waves in the theory of thermoviscoelastic materials with voids. *J. Therm. Stresses* **39**(2), 142–155 (2016)
29. Graff, K.F., Pao, Y-H.: The effects of couple-stresses on the propagation and reflection of plane waves in an elastic half-space. *J. Sound Vib.* **6**(2), 217–229 (1967)
30. Parfitt, V.R., Eringen, A.C.: Reflection of plane waves from the flat boundary of a micropolar elastic half-space. *J. Acoust. Soc. Am.* **45**(5), 1258–1272 (1969)
31. Gourgiotis, P.A., Georgiadis, H.G., Neocleous, I.: On the reflection of waves in half-spaces of microstructured materials governed by dipolar gradient elasticity. *Wave Motion* **50**(3), 437–455 (2013)
32. Eringen, A.C.: *Nonlocal Continuum Field Theories*. Springer, New York (2002)
33. Eringen, A.C.: Plane waves in nonlocal micropolar elasticity. *Int. J. Eng. Sci.* **22**(8–10), 1113–1121 (1984)
34. Borchardt, R.D.: *Viscoelastic Waves in Layered Media*. Cambridge Univ. Press, Cambridge (2009)
35. Ciarletta, M., Sumbatyan, M.A.: Reflection of plane waves by the free boundary of a porous elastic half-space. *J. Sound Vib.* **259**(2), 253–264 (2003)
36. Ewing, W.M., Jardetzky, W.S., Press, F.: *Elastic Waves in Layered Media*. McGraw-Hill, New York (1957)
37. Achenbach, J.D.: *Wave Propagation in Elastic Solids*. North-Holland, New York (1976)